



$\bar{B}_s \rightarrow f_0(980)$ form factors and the width effect from light-cone sum rules

Shan Cheng^a , Jian-Ming Shen^b

School of Physics and Electronics, Hunan University, Changsha 410082, People's Republic of China

Received: 20 February 2020 / Accepted: 6 June 2020 / Published online: 18 June 2020
© The Author(s) 2020

Abstract In this paper we calculate the $\bar{B}_s \rightarrow f_0(980)$ form factors from light-cone sum rules with B meson DAs. With adopting the quark–antiquark configuration of light scalar mesons, the high twist two-particle and the three-particle contributions are found to be $\sim 25\%$ individual, and totally they give about 50% correction to certain form factors in the considered energy regions. We further explore the light-cone sum rules approach to study the S -wave $\bar{B}_s \rightarrow KK$ form factors, the $f_0 + f'_0 + f''_0$ resonance model is proposed and the result shows that the background effect from $f'_0 + f''_0$ accounts $\sim 5\%$. As a by-product, we extract the strong coupling $|g_{f_0 KK}| = 1.08^{+0.05}_{-0.14}$ GeV with taking the $\bar{B}_s \rightarrow f_0(980)$ form factors calculated previous under the narrow width approximation.

1 Introduction

Form factor is a fundamental physical quantum in effective field theory (EFT), with including both the long distance (LD) and short distance (SD) physics. In order to extract the Cabibbo–Kobayashi–Maskawa (CKM) matrix elements, reliably, in the semileptonic B decay processes, the precise calculations of the relevant form factors are inevitable. The heavy-to-light form factors are calculated by different approaches, in which the lattice QCD (LQCD) gives the reliable simulations in the low recoiled regions [1, 2], while in the large and full recoiled regions, the QCD-based analytical approaches like the light-cone sum rules (LCSRs) [3–14] and the perturbative QCD (PQCD) [15–21] are applied.

There are many successful calculations for the heavy-to-light transition form factors with the final state being a pseudoscalar (P) or a vector (V) meson. While to our knowledge, the transition form factors with light scalar (S) meson final

state are not understood well so far due to the unclear underlying structure and the large width effect. It has been suggested that the scalar mesons with masses below or near 1 GeV (the isoscalar $\sigma/f_0(500)$ and $f_0(980)$, the isodoublet κ , and the isovector a_0) form a $SU(3)$ flavor nonet, and the scalar mesons with masses around 1.5 GeV ($f_0(1370)$, $a_0(1450)$, $K_0^*(1430)$ and $f_0(1500)$) form the other one. The combined analysis based on orbital angular momentum [22–24] and data [25–27] implies that the heavier nonet states favour the quark–antiquark configuration replenished with some possible gluon content. From the spectral analysis, there is not a general agreement on the underlying assignments of the scalar mesons in the lighter nonet, like $f_0(980)$. Pictures like tetra-quark [22, 23, 28, 29], gluonball [30], hybrid state [31] and molecule state [32] are all discussed, in which the tetra-quark assignment is more favorite nowadays. The case is different in the $B \rightarrow f_0(980)$ decays when $f_0(980)$ is energetic and the process happens with large recoiling, where the conventional quark–antiquark assignment is the favorite one since the possibility to form a tetra-quark state is power suppressed with comparing to the state of quark pair [24]. So in this work, with the main purpose to calculate the heavy-to-light transition form factors, we would take the usual quark–antiquark nature of $f_0(980)$, and postpone the tetra-quark study somewhere else.

Some attempts are carried out to calculate the $B \rightarrow S$ transition form factors from LCSRs with scalar mesons distribution amplitudes (DAs) [33–36]. We comment that these work considered only the scalar mesons in the heavier nonet, and their accuracy is debatable since some important informations of the input DAs, such as the standard conformal partial expansion and the width effect, are still missing. In this paper, with taking the $\bar{s}s$ configuration of $f_0(980)$, we suggest to study the $\bar{B}_s \rightarrow f_0(980)$ form factor from the alternative LCSRs with B meson DAs. Although the width

^a e-mail: scheng@hnu.edu.cn (corresponding author)

^b e-mail: shenjm@hnu.edu.cn

of $f_0(980)$ is suppressed by the phase space¹, we would like to access the width effect by applying the approach proposed to calculate $B \rightarrow \pi\pi, K\pi$ form factors [12, 13], with substituting the isovector $\pi\pi$ state by the scalar isoscalar KK state.

The rest of this paper is organised as follows. In Sect. 2 we revisit and update the mass and the decay constant of $f_0(980)$ in the two-point QCD sum rules. Sections 3 and 4 are the main parts of this paper, where we present the LCSRs calculation for $\bar{B}_s \rightarrow f_0(980)$ form factors and generalizes it to study the S -wave $\bar{B}_s \rightarrow KK$ form factors, respectively. We summary in Sect. 5. The coefficients in three-particle corrections from B meson LCDAs are complemented in Appendix B.

2 σ and $f_0(980)$ in the QCD sum rules revisited

QCD sum rules [39] is a powerful tool to study hadron spectrum. For the meson with $I^G(J^{PC}) = 0^+(0^{++})$, the scalar isoscalar currents include both $J^n = \bar{n}n = \frac{1}{\sqrt{2}}(\bar{u}u + \bar{d}d)$ and $J^s = \bar{s}s$. We start with the two-point correlation function

$$\Pi_{2\text{pSRs}}(q) = i \int d^4x e^{iqx} \langle 0 | T \{ J^s(x), J^s(0) \} | 0 \rangle. \tag{1}$$

Although the data of $D_s^+ \rightarrow f_0\pi^+$ indicates $f_0(980)$ may be dominated by the $\bar{s}s$ component, much more measurements [40–49], especially the comparable branching ratios between $B \rightarrow f_0(980) \rightarrow \pi\pi$ and $B \rightarrow f_0(980) \rightarrow KK$ [50], support a mixing between f_0 and σ :

$$\begin{aligned} |f_0(980)\rangle &= |s\bar{s}\rangle \cos\theta + |n\bar{n}\rangle \sin\theta, \\ |\sigma(500)\rangle &= -|s\bar{s}\rangle \sin\theta + |n\bar{n}\rangle \cos\theta. \end{aligned} \tag{2}$$

The mixing implies that f_0 and σ should be treated separately, and in the basis of flavour, two decay constants are needed to describe each of them,

$$\begin{aligned} \langle f_0 | \bar{u}u | 0 \rangle &= \frac{1}{\sqrt{2}} m_{f_0} \bar{f}_{f_0}^n, & \langle f_0 | \bar{s}s | 0 \rangle &= m_{f_0} \bar{f}_{f_0}^s, \\ \langle \sigma | \bar{u}u | 0 \rangle &= \frac{1}{\sqrt{2}} m_\sigma \bar{f}_\sigma^n, & \langle \sigma | \bar{s}s | 0 \rangle &= m_\sigma \bar{f}_\sigma^s. \end{aligned} \tag{3}$$

The neutral scalar meson can not be produced via the vector current because f_S is vanished in the $SU(3)$ /isospin limit with the charge conjugation invariance and the conservation of vector current.

¹ In fact the width of f_0 is smaller than it of ρ meson. It should be stressed that the width effect in $B \rightarrow \rho$ transition is usually neglected because in the experimental analysis the ρ meson is identified by the P-wave $\pi\pi$ signal when the dipion invariant mass locates in the ρ -pole region [37, 38]. This makes the narrow-width treatment for $B \rightarrow \rho$ form factor from LCSRs being consistent with the experimental measurement.

The basic idea of QCD sum rules is to calculate independently for the correlation function in twofold ways: the QCD calculation at quark-gluon level in the Euclidean momenta space, and the summing of intermediate states from the view of hadron. The QCD calculation in the negative half plane of q^2 is guaranteed by the operator-product-expansion (OPE) technology, and the correlation function is then written in terms of various vacuum condensates. On the other hand, the average distance between two coordinate points (0 and x in Eq. 1) grows when q^2 shifting from large negative to positive values, and then the LD quark-gluon interaction forms the hadrons [5]. In this way, the correlation function can be expressed as the sum of contributions from all possible intermediate states in the positive half-plane, with possible subtractions. The accuracy of LCSRs approach is mainly depended on how to match the QCD calculation to the hadron spectral analysis, in more word is how to take the quark-hadron duality in the dispersion relation to eliminate the contributions from excited and continuum states.

By inserting a complete set of intermediate states $|n\rangle$, the unitarity relation ($q^2 > 0$) of the correlation function reads as,

$$\begin{aligned} 2 \text{Im} \Pi_{2\text{pSRs}}(q) &= \sum_n \langle 0 | J^s(x) | n \rangle \langle n | J^s(0) | 0 \rangle d\tau_n (2\pi)^4 \delta(q - p_n), \end{aligned} \tag{4}$$

where $d\tau_n$ denotes the phase space of each state $|n\rangle$, like $\sigma, f_0(980)$ and their excited states. We are now interesting in $f_0(980)$ which enters in the two-point sum rules as the first excited state with the ground state σ , so we include both them in the hadron inserting and take the threshold s_0 to truncate the higher excited states. After applying the dispersion relation and employing the quark-hadron duality, the matching between quark amplitude and the hadron spectral analysis is taken as

$$\sum_{S=\sigma, f_0} \frac{m_S^2 (\bar{f}_S^s)^2}{(m_S^2 - q^2)} = \frac{1}{\pi} \int_0^{s_0} ds \frac{\text{Im} \Pi_{2\text{pSRs}}^{\text{OPE}}(s)}{s - q^2}, \tag{5}$$

where $\Pi_{2\text{pSRs}}^{\text{OPE}}(s)$ is the OPE result for the correlation function. In order to improve the convergence of OPE calculation and suppress the contributions from high excited states and continuum spectrums, we apply the Borel transformation to both sides of Eq. 5. The result is quoted [51, 52] as follow, with α_s to one-loop order and the vacuum condensate terms up to dimension six,

$$\begin{aligned} \sum_{S=\sigma, f_0} m_S^2 (\bar{f}_S^s(\mu_0))^2 e^{-m_S^2/M^2} \left(\frac{\alpha_s(\mu_0)}{\alpha_s(M)} \right)^{2/\beta_1} &= \frac{3}{8\pi^2} M^4 \left[1 + h(1) \right] f(1) + \frac{1}{8} \left\langle \frac{\alpha_s G^2}{\pi} \right\rangle + 3m_s \langle \bar{s}s \rangle \end{aligned}$$

$$-\frac{1}{M^2} \left[m_s \langle \bar{s} g_s \sigma \cdot G s \rangle - \frac{2}{3} \pi \alpha_s \langle \bar{s} \gamma_\mu \lambda^a s \bar{u} \gamma^\mu \lambda^a s \rangle - \pi \alpha_s \langle \bar{s} \sigma_{\mu\nu} \lambda^a s \bar{s} \sigma^{\mu\nu} \lambda^a s \rangle \right]. \tag{6}$$

The functions defined in the perturbative terms are

$$f(n) = 1 - e^{-\frac{s_0}{M^2}} \left[1 + \frac{s_0}{M^2} + \frac{1}{2} \left(\frac{s_0}{M^2} \right)^2 + \frac{1}{n!} \left(\frac{s_0}{M^2} \right)^n \right],$$

$$I(n) = \int_{e^{-\frac{s_0}{M^2}}}^1 dt \ln^n t \ln(-\ln t),$$

$$h(n) = \frac{\alpha_s(M)}{\pi} \left(\frac{17}{3} + 2 \frac{I(1)}{f(1)} - 2 \ln \frac{M^2}{\mu^2} \right). \tag{7}$$

We use the two-loop expression for strong coupling [50],

$$\alpha_s(\mu) = \frac{\pi}{2\beta_1 \log(\mu/\Lambda)} \left(1 - \frac{\beta_2 \log(2 \log(\mu/\Lambda))}{\beta_1^2 \log(\mu/\Lambda)} \right), \tag{8}$$

with the evolution kernels $\beta_1 = (33 - 2n_f)/12$ and $\beta_2 = (153 - 19n_f)/24$. The hadronic scale Λ is set to reproduce $\alpha_s(m_Z) = 0.118$ and $\alpha_s(1 \text{ GeV}) = 0.474$, and written in terms of step function

$$\Lambda^{(n_f)} = \text{Which} [n_f = 3, 0.332, n_f = 4, 0.292, n_f = 5, 0.210]. \tag{9}$$

The input values for the nonperturbative vacuum condensates at default scale 1 GeV are taken as [53–55]:

$$\begin{aligned} \langle \bar{u}u \rangle &= (-0.25 \text{ GeV})^3, & \langle \bar{s}s \rangle &= 0.8 \langle \bar{u}u \rangle, \\ \langle g_s \bar{q} \sigma \cdot G q \rangle &= -0.8 \langle \bar{q}q \rangle, \\ \langle \alpha_s / \pi G_{\mu\nu}^a G^{a\mu\nu} \rangle &= 0.012 \text{ GeV}^4, \\ \langle \bar{q} \gamma_\mu \lambda^a q \bar{q} \gamma^\mu \lambda^a q \rangle &= -\frac{16}{9} \langle \bar{q}q \rangle^2, \\ \langle \bar{q} \sigma_{\mu\nu} \lambda^a q \bar{q} \sigma^{\mu\nu} \lambda^a q \rangle &= -\frac{3}{4} \langle \bar{q}q \rangle^2. \end{aligned} \tag{10}$$

The light quark masses are estimated as the “current-quark” masses in the $\overline{\text{MS}}$ ($\mu = 1 \text{ GeV}$) scheme [50],

$$m_s = 0.125 \text{ GeV}. \tag{11}$$

We also consider the running of parameters with one-loop accuracy [56–59],

$$\begin{aligned} m_q(\mu) &= m_q(\mu_0) \left(\frac{\alpha_s(\mu_0)}{\alpha_s(\mu)} \right)^{-1/\beta_1}, \\ \langle \bar{q}q \rangle_\mu &= \langle \bar{q}q \rangle_{\mu_0} \left(\frac{\alpha_s(\mu_0)}{\alpha_s(\mu)} \right)^{1/\beta_1}, \\ \langle \alpha_s G^2 \rangle_\mu &= \langle \alpha_s G^2 \rangle_{\mu_0}, \\ \langle g_s \bar{q} \sigma \cdot G q \rangle_\mu &= \langle g_s \bar{q} \sigma \cdot G q \rangle_{\mu_0} \left(\frac{\alpha_s(\mu_0)}{\alpha_s(\mu)} \right)^{-1/(6\beta_1)}. \end{aligned} \tag{12}$$

Differentiating both sides of Eq. 6 by the Borel mass we obtain an auxiliary sum rules,

$$\begin{aligned} \sum_{s=\sigma, f_0} \frac{m_s^4 (\bar{f}_s^s(\mu_0))^2 e^{-m_s^2/M^2}}{m_s^2 (\bar{f}_s^s(\mu_0))^2 e^{-m_s^2/M^2}} \\ = \frac{2M^2 [1 + h(2)] f(2) + \frac{8\pi^2}{3} \frac{68\pi\alpha_s}{27M^4} \langle \bar{s}s \rangle^2}{[1 + h(1)] f(1) + \frac{8\pi^2}{3} \left[\frac{1}{8M^4} \langle \alpha_s G^2 \rangle - \frac{68\pi\alpha_s}{27M^6} \langle \bar{s}s \rangle^2 \right]}, \end{aligned} \tag{13}$$

which is further used, together with the renormalization-improved sum rules in Eq. 6, to fit the masses and decay constants of σ and f_0 . The terms proportional to quark mass on the right hand side are neglected in Eq. 13.

The Borel mass is fixed by the rule of thumb that the contribution from high dimension condensate terms is no larger than twenty percents in the truncated OPE, and simultaneously the contribution from excited and continuum states is smaller than thirty percents when summing up the hadrons. The threshold value s_0 is usually close to the outset of the first higher excited state with the same quantum number, then a certain vicinity can be expected, we determine it with considering the maximal stability of physical quantities once the Borel mass has been set down. Within the interval $M^2 = 1.0 \pm 0.1 \text{ GeV}^2$ at the fixed threshold value $s_0 = 2.0 \pm 0.2 \text{ GeV}^2$ which is slightly larger than the one used in [28, 29] because we are discussing the $s\bar{s}$ current, we do the combined quadratic fit to both sides of Eqs. (6, 13), and obtain

$$\begin{aligned} m_{f_0} &= (985 \pm 122) \text{ MeV}, \\ m_\sigma &= (439 \pm 304) \text{ MeV}, \\ \bar{f}_{f_0}^s(1 \text{ GeV}) &= (358 \pm 4) \text{ MeV}, \\ \bar{f}_\sigma^s(1 \text{ GeV}) &\sim 0. \end{aligned} \tag{14}$$

The s -flavor decay constant of f_0 agrees with the prediction $\bar{f}_{f_0}^s = (370 \pm 20) \text{ MeV}$ obtained under the assumption that $f_0(980)$ and $f_0(1500)$ are the lowest scalar states with $\bar{s}s$ assignment [24]. The nearly zero s -flavor decay constant of σ indicates that $f_0(980)$ is the lowest state in the channel with scalar isoscalar current J^s , standing by which we reevaluate the sum rules in Eqs. (6, 13) by considering only the f_0 state, and obtain the same result for m_{f_0} and $\bar{f}_{f_0}^s$ as listed in Eq. 14.

3 $\bar{B}_s \rightarrow f_0$ form factors from the LCSRs

The approach of LCSRs with B meson DAs was proposed to calculate the $B \rightarrow P, V$ form factors [9], in this section we implement it to calculate the $\bar{B}_s \rightarrow f_0$ form factors.

As we demonstrated in the last section that the scalar isoscalar current $\bar{s}s$ coupling to σ is nearly zero, so it would be reasonable to consider $f_0(980)$ as the lowest scalar state in B_s decays. This consideration is also supported by the fact that no evidence of σ is observed in the B decays so far [60]. Let's consider another correlation function

$$\Pi_v(p, q) = i \int d^4x e^{ip \cdot x} \langle 0 | T \{ J^S(x), J_v^{\mathcal{I}}(0) \} | \bar{B}_s(p+q) \rangle, \tag{15}$$

with the weak current $J_v^{\mathcal{I}} = \bar{s} \Gamma_v^{\mathcal{I}} b$. The indicator $\mathcal{I} = A, T$ correspond to the gamma matrices $\Gamma_v^A = \gamma_v \gamma_5$ and $\Gamma_v^T = \sigma_{\nu\mu} \gamma_5 q^\mu$, respectively.² The heavy-to-light current is reduced to the light quark current after transiting to the heavy quark effective theory (HQET), and the correlation function is modified to

$$\tilde{\Pi}_v(p, \tilde{q}) = i \int d^4x e^{ip \cdot x} \langle 0 | T \{ J^S(x), \tilde{J}_v^{\mathcal{I}}(0) \} | \bar{B}_{s,v}(p+\tilde{q}) \rangle. \tag{16}$$

We use the notations p to denote the momentum carried by the scalar isoscalar current J^S , and $\tilde{q} = q - m_b v$ for the effective current $\tilde{J}_v^{\mathcal{I}} = \bar{s} \Gamma_v^{\mathcal{I}} h_v$. In the rest frame the effective b -quark field is defined by $h_v(x) = e^{im_b v x} b(x)$ with the unit vector $v = (1, 0, 0, 0)$, and $|\bar{B}_s(p+q)\rangle = |\bar{B}_{s,v}(p+\tilde{q})\rangle$ holds up to the $\mathcal{O}(1/m_b)$ accuracy. We would discuss in the intervals $|p^2|, |\tilde{q}^2| \gg \Lambda_{QCD}^2, (m_{B_s} - m_b)^2$ where the correlation function does not fluctuate violently and the OPE calculation works well.

In the correlation function, the same flavour quark fields with small displacement can be contracted in the form of quark propagator,

$$s_s(x, 0, m_s) = \int \frac{d^4p}{(2\pi)^4} e^{-ipx} \int_0^1 du G_{\mu\nu}(ux) \cdot \left[\frac{ux^\mu \gamma^\nu}{p^2 - m_s^2} - \frac{(\not{p} + m_s) \sigma_{\mu\nu}}{2(p^2 - m_s^2)^2} \right], \tag{17}$$

in which the first term is the freedom part in the QCD limit, and the second term respects the soft one-gluon correction. Two-particle and three-particle DAs of B_s meson are defined as [61],

$$\begin{aligned} &\langle 0 | \bar{s}_\alpha(x) h_{v\beta}(0) | \bar{B}_{s,v} \rangle \\ &= -\frac{if_{B_s} m_{B_s}}{4} \int_0^\infty d\omega e^{-i\omega v \cdot x} \\ &\left[(1 + \not{v}) \left\{ [\phi_+(\omega) + x^2 g_+(\omega)] \right. \right. \\ &\quad \left. \left. - \frac{[\phi_+(\omega) - \phi_-(\omega) + x^2 (g_+(\omega) - g_-(\omega))]}{2v \cdot x} \right\} \not{x} \gamma_5 \right]_{\beta\alpha}, \tag{18} \end{aligned}$$

$$\langle 0 | \bar{s}_\alpha(x) G_{\rho\delta}(ux) h_{v\beta}(0) | \bar{B}_{s,v} \rangle$$

² We use the convention $\sigma_{\mu\nu} = \frac{i}{2}(\gamma_\mu \gamma_\nu - \gamma_\nu \gamma_\mu)$.

$$\begin{aligned} &= \frac{f_{B_s} m_{B_s}}{4} \int_0^\infty d\omega \int_0^\infty d\zeta e^{-i(\omega+u\zeta)v \cdot x} \left[(1 + \not{v}) \right. \\ &\cdot \left\{ (v_\rho \gamma_\delta - v_\delta \gamma_\rho) [\Psi_A(\omega, \zeta) - \Psi_V(\omega, \zeta)] - i\sigma_{\rho\delta} \Psi_V(\omega, \zeta) \right. \\ &- \left(\frac{x_\rho v_\delta - x_\delta v_\rho}{v \cdot x} \right) X_A(\omega, \zeta) \\ &+ \left(\frac{x_\rho \gamma_\delta - x_\delta \gamma_\rho}{v \cdot x} \right) [Y_A(\omega, \zeta) + W(\omega, \zeta)] \\ &+ i\epsilon_{\rho\delta\alpha\beta} \frac{x^\alpha v^\beta}{v \cdot x} \gamma_5 \tilde{X}_A(\omega, \zeta) - i\epsilon_{\rho\delta\alpha\beta} \frac{x^\alpha \gamma^\beta}{v \cdot x} \gamma_5 \tilde{Y}_A(\omega, \zeta) \\ &- \left(\frac{x_\rho v_\delta - x_\delta v_\rho}{v \cdot x} \right) \frac{\not{x}}{v \cdot x} W(\omega, \zeta) \\ &\left. \left. + \left(\frac{x_\rho \gamma_\delta - x_\delta \gamma_\rho}{v \cdot x} \right) \frac{\not{x}}{v \cdot x} Z(\omega, \zeta) \right\} \right]_{\beta\alpha}, \tag{19} \end{aligned}$$

respectively. Two variables ω and ζ are introduced to represent the plus components of light quark and the gluon momentum, respectively. The path-ordered gauge factor is always underlined in the matrix element sandwiched between meson state and vacuum. Recently, the renormalization group equations (RGE) are resolved in the N_C limit for three-particle DAs [62], and the models are suggested for the higher-twist B meson DAs [63], following which the power suppressed correction are supplemented to $B \rightarrow P, V, \gamma$ form factors [13, 63–66]. The Lorentz definition in Eqs. (18, 19) should not be confused with the definite twist definition of LCDAs, we collect their relations, as well as the general model for the later one in Appendix A.

The definition of $\bar{B}_s \rightarrow S$ transition form factors is quoted as [67, 68]

$$\begin{aligned} &\langle S(p) | J_v^A(0) | \bar{B}_s(p+q) \rangle \\ &= -i[\mathcal{F}_+(q^2) p_v + \mathcal{F}_-(q^2) q_v] \\ &= -i\mathcal{F}_1(q^2) \left[(2p+q)_v - \frac{m_{B_s}^2 - m_S^2}{q^2} q_v \right] \\ &\quad - i\mathcal{F}_0(q^2) \frac{m_{B_s}^2 - m_S^2}{q^2} q_v, \tag{20} \end{aligned}$$

$$\begin{aligned} &\langle S(p) | J_v^T(0) | \bar{B}_s(p+q) \rangle \\ &= -\frac{\mathcal{F}_T(q^2)}{m_{B_s} + m_S} \left[q^2 (2p+q)_v - (m_{B_s}^2 - m_S^2) q_v \right]. \tag{21} \end{aligned}$$

The following relations are suggested for the form factors associated with axial-vector current in Eq. 20,

$$\begin{aligned} &\mathcal{F}_1(q^2) = \frac{\mathcal{F}_+(q^2)}{2}, \tag{22} \\ &\mathcal{F}_0(q^2) \frac{(m_{B_s}^2 - m_S^2)}{q^2} \\ &= \mathcal{F}_-(q^2) + \frac{\mathcal{F}_+(q^2) (m_{B_s}^2 - m_S^2 - q^2)}{2}. \tag{23} \end{aligned}$$

We calculate the correlation function in Eq. 16 under the narrow width approximation, obtain the LCSRs result for

$\bar{B}_s \rightarrow f_0(980)$ form factors,

$$\begin{aligned}
 m_{f_0} \bar{f}_{f_0}^s \mathcal{F}_+^{\bar{B}_s \rightarrow f_0}(q^2) e^{-m_{f_0}^2/M^2} &= f_{B_s} m_{B_s}^2 \left\{ \int_0^{\sigma_0} d\sigma e^{-s_q/M^2} \left[\phi_+(\sigma m_{B_s}) \right. \right. \\
 &\quad \left. \left. - \frac{\bar{\phi}_\pm(\sigma m_{B_s})}{\bar{\sigma} m_{B_s}} - \frac{8\bar{\sigma}^2 m_{B_s}^2 g_+(\sigma m_{B_s})}{(\bar{\sigma}^2 m_{B_s}^2 - q^2)^2} \right. \right. \\
 &\quad \left. \left. - \frac{4\bar{\sigma} g'_+(\sigma m_{B_s})}{(\bar{\sigma}^2 m_{B_s}^2 - q^2)} \right] + \Delta\mathcal{F}_+(q^2, s_0, M^2) \right\}, \tag{24}
 \end{aligned}$$

$$\begin{aligned}
 m_{f_0} \bar{f}_{f_0}^s \mathcal{F}_-^{\bar{B}_s \rightarrow f_0}(q^2) e^{-m_{f_0}^2/M^2} &= f_{B_s} m_{B_s}^2 \left\{ \int_0^{\sigma_0} d\sigma e^{-s_q/M^2} \left[-\frac{\sigma \phi_+(\sigma m_{B_s})}{\bar{\sigma}} \right. \right. \\
 &\quad \left. \left. - \frac{\bar{\phi}_\pm(\sigma m_{B_s})}{\bar{\sigma} m_{B_s}} + \frac{8\bar{\sigma} \sigma m_{B_s}^2 g_+(\sigma m_{B_s})}{(\bar{\sigma}^2 m_{B_s}^2 - q^2)^2} \right. \right. \\
 &\quad \left. \left. + \frac{4\sigma g'_+(\sigma m_{B_s})}{(\bar{\sigma}^2 m_{B_s}^2 - q^2)} \right] + \Delta\mathcal{F}_-(q^2, s_0, M^2) \right\}, \tag{25}
 \end{aligned}$$

$$\begin{aligned}
 \frac{2m_{f_0} \bar{f}_{f_0}^s}{m_{B_s} + m_{f_0}} \mathcal{F}_T^{\bar{B}_s \rightarrow f_0}(q^2) e^{-m_{f_0}^2/M^2} &= f_{B_s} m_{B_s}^2 \left\{ \int_0^{\sigma_0} d\sigma e^{-s_q/M^2} \right. \\
 &\quad \left[\frac{\phi_+(\sigma m_{B_s})}{\bar{\sigma} m_{B_s}} - \frac{8\bar{\sigma} m_{B_s} g_+(\sigma m_{B_s})}{(\bar{\sigma}^2 m_{B_s}^2 - q^2)^2} \right. \\
 &\quad \left. \left. - \frac{4g'_+(\sigma m_{B_s})}{m_{B_s}(\bar{\sigma}^2 m_{B_s}^2 - q^2)} \right] \right. \\
 &\quad \left. + \frac{1}{m_{B_s}^2 - m_{f_0}^2 - q^2} \Delta\mathcal{F}_{T,q}(q^2, s_0, M^2) \right\}. \tag{26}
 \end{aligned}$$

The contributions proportional to light quark mass m_s are not shown explicitly above. The dimensionless variable $\sigma \equiv \omega/m_{B_s}$ is the longitudinal momentum fraction of the light quark inside \bar{B}_s meson, and the virtuality of internal quark is $s_q = m_{B_s}^2 \sigma - (q^2 \sigma - m_s^2)/\bar{\sigma}$. To process the calculation, we have defined an auxiliary distribution

$$\bar{\phi}_\pm(\omega) \equiv \int_0^\omega d\tau [\phi_+(\tau) - \phi_-(\tau)], \tag{27}$$

with the boundary conditions $\bar{\phi}_\pm(0) = \bar{\phi}_\pm(\infty) = 0$. The derivation is $g'_+(\sigma m_{B_s}) = (d/d\sigma) g_+(\sigma m_{B_s})$. We give several comments in orders:

- (i) With taking into account the quark mass effect, our results shown in Eqs. (24, 25) consist with the calculations of $B \rightarrow D_0^*$ form factors [69].
- (ii) $\mathcal{F}_{T,p}(q^2)$ and $\mathcal{F}_{T,q}(q^2)$ are obtained by matching the coefficients associated with different Lorentz structures (say, p_ν and q_ν , respectively) with the matrix element sandwiched by the tensor current. In principle, they should be equal to each other when considering only

the two-particle DAs,³ so we use the unified notation $\mathcal{F}_T(q^2)$.

- (iii) In the heavy quark limit $\sigma \rightarrow 0$, we reproduce the relations $\mathcal{F}_+(0) = 2m_{B_s}/(m_{B_s} + m_s) \mathcal{F}_T(0)$ and $\mathcal{F}_-(0) = 0$ at the full recoiled point.

Multiplying both sides of Eq. 20 by q^ν , we derive the matrix elements deduced by the pseudo-scalar current $J^P = im_b \bar{s} \gamma_5 b$,

$$\langle S(p) | J^P(0) | B_s(p+q) \rangle = (m_{B_s}^2 - m_s^2) \mathcal{F}_0(q^2), \tag{28}$$

which suggests another sum rules,

$$\begin{aligned}
 m_{f_0} \bar{f}_{f_0}^s (m_{B_s}^2 - m_{f_0}^2) \mathcal{F}_0^{\bar{B}_s \rightarrow f_0}(q^2) e^{-m_{f_0}^2/M^2} &= f_{B_s} m_{B_s}^2 m_b \left\{ \int_0^{\sigma_0} d\sigma e^{-s_q/M^2} \right. \\
 &\quad \left[\frac{(\bar{\sigma}^2 m_{B_s}^2 - q^2) \phi_+(\sigma m_{B_s})}{2\bar{\sigma}^2 m_{B_s}} - \frac{3\bar{\phi}_\pm(\sigma m_{B_s})}{\bar{\sigma}} \right. \\
 &\quad \left. - \left[2\bar{\sigma} m_{f_0}^2 - 2\sigma q^2 + (1 - 2\sigma)(m_{B_s}^2 - m_{f_0}^2 - q^2) \right] \right. \\
 &\quad \left. \cdot \left(\frac{\bar{\sigma} m_{B_s} g_+(\sigma m_{B_s})}{(\bar{\sigma}^2 m_{B_s}^2 - q^2)^2} + \frac{g'_+(\sigma m_{B_s})}{2m_{B_s}(\bar{\sigma}^2 m_{B_s}^2 - q^2)} \right) \right. \\
 &\quad \left. + \Delta\mathcal{F}_0(q^2, s_0, M^2) \right\}. \tag{29}
 \end{aligned}$$

We remark that Eq. 28 is established on the heavy quark limit, so the new LCSRs in Eq. 29 can be used to estimate how well does the heavy quark expansion work by comparing it with the original LCSRs in Eqs. (24, 25).

The contributions from three-particle DAs of B meson are arranged in an universal form

$$\begin{aligned}
 \Delta\mathcal{F}_i(q^2, s_0, M^2) &= \int_0^{\sigma_0} d\sigma e^{-s_q/M^2} \left(-I_{1,i}(\sigma) + \frac{I_{2,i}(\sigma)}{M^2} - \frac{I_{3,i}(\sigma)}{2M^4} \right) \\
 &\quad + \frac{e^{-s_0/M^2}}{m_{B_s}^2} \left\{ \eta(\sigma) \left[I_{2,i}(\sigma) - \frac{I_{3,i}(\sigma)}{2} \left(\frac{1}{M^2} + \frac{1}{m_{B_s}^2} \frac{d\eta}{d\sigma} \right) \right. \right. \\
 &\quad \left. \left. - \frac{\eta}{2m_{B_s}^2} \frac{dI_{3,i}(\sigma)}{d\sigma} \right] \right\} \Big|_{\sigma=\sigma_0}, \tag{30}
 \end{aligned}$$

where the dimensionless variable $\eta = (\bar{\sigma}^2 m_{B_s}^2)/(\bar{\sigma}^2 m_{B_s}^2 - q^2 + m^2)$ can be understood as the ratio between the minimal virtuality of the b quark field and the maximal virtuality carried by the internal light quark. The integral over the three-particle DAs is written as

$$\begin{aligned}
 I_{N,i}(\sigma) &= \frac{1}{\bar{\sigma}^N} \int_0^{\sigma m_{B_s}} d\omega \int_{\sigma m_{B_s} - \omega}^\infty \frac{d\zeta}{\zeta} \\
 &\quad \cdot \left\{ C_{N,i}^{\Psi_A}(\sigma, u, q^2) \Psi_A(\omega, \zeta) \right\}
 \end{aligned}$$

³ Because the coefficients of three-particle correlation in $\Delta\mathcal{F}_{T,p}$ may have the $1/q^2$ factor, we would take $\Delta\mathcal{F}_{T,q}$ for this part contribution in numerical analysis.

$$\begin{aligned}
 &+C_{N,i}^{\Psi_V}(\sigma, u, q^2) \Psi_V(\omega, \zeta) \\
 &+C_{N,i}^{\bar{X}_A}(\sigma, u, q^2) \bar{X}_A(\omega, \zeta) \\
 &+C_{N,i}^{\bar{Y}_A}(\sigma, u, q^2) [\bar{Y}_A(\omega, \zeta) + \bar{W}(\omega, \zeta)] \\
 &+C_{N,i}^{\bar{\bar{X}}_A}(\sigma, u, q^2) \bar{\bar{X}}_A(\omega, \zeta) \\
 &+C_{N,i}^{\bar{\bar{Y}}_A}(\sigma, u, q^2) \bar{\bar{Y}}_A(\omega, \zeta) \\
 &+C_{N,i}^{\bar{\bar{W}}}(\sigma, u, q^2) \bar{\bar{W}}(\omega, \zeta) \\
 &+C_{N,i}^{\bar{\bar{Z}}}(\sigma, u, q^2) \bar{\bar{Z}}(\omega, \zeta) \Big|_{u=(\sigma m_{B_s} - \omega)/\zeta}, \quad (31)
 \end{aligned}$$

here another two auxiliary distributions are introduced for $\bar{X}_A, \bar{Y}_A, \bar{W}, \bar{\bar{X}}_A, \bar{\bar{Y}}_A$ and $\bar{\bar{W}}, \bar{\bar{Z}}$,

$$\bar{f} \equiv \int_0^\omega d\tau f(\tau, \zeta), \quad \bar{\bar{f}} \equiv \int_0^\omega d\tau \int_0^\zeta d\tau' f(\tau, \tau'). \quad (32)$$

The lower indicator $N = 1, 2, 3$ stands for the power of Borel mass $M^{-2(N-1)}$ premultiplied with the integrals, the coefficients $C_{N,i}$ associated to each three-particle DA are presented in Appendix B.

We take $m_b(m_b) = 4.2$ GeV for b quark mass in the typical $\overline{\text{MS}}$ scheme, and use $f_{B_s} = 0.242$ GeV obtained from lattice QCD [70] and two-point QCD sum rules [71]. The inverse moment of \bar{B}_s DAs is chosen in the interval $\lambda_{\bar{B}_s} = 450 \pm 50$ MeV, a little bit smaller than the conventional value 500 ± 50 MeV, by considering the possible next-to-leading-order radiative correction effects⁴ [11, 72]. The same ballpark of the LCSR parameters, say, $M^2 = 1.0 \pm 0.1$ GeV² and $s_0 = 2.0 \pm 0.2$ GeV², are used here as in the two-point sum rules in the last section, with which the OPE convergence is automatically manifested by the relative small three-particle DAs contribution $\mathcal{F}^{3p}(Q^2)/\mathcal{F}^{2p}(Q^2) \lesssim 30\%$ for $Q^2 \in [0, 5]$ GeV². We plot in Fig. 1 for the $\bar{B}_s \rightarrow f_0$ form factors obtained under the narrow width approximation, where the lightgray shadows reveal the total uncertainty came from the inverse moment $\lambda_{\bar{B}_s}$ and the LCSR parameters. The high twist B meson DAs with two-particle configuration (g_+) give about 25% decrease to \mathcal{F}_+ and \mathcal{F}_T , about 20% increase to \mathcal{F}_- , the tiny change of \mathcal{F}_0 from g_+ can be understood by the interplay between the negative correction for \mathcal{F}_+ and the positive correction for \mathcal{F}_- . The three-particle \bar{B}_s DAs bring another 25% decrease and increase to \mathcal{F}_T and \mathcal{F}_- , respectively, while its corrections to \mathcal{F}_+ and \mathcal{F}_0 are tiny, indicating that the heavy quark limit is broken with considering the three-particle DAs correction. We compare our result for $\bar{B}_s \rightarrow f_0$ form factors with other methods in Table 1.

⁴ Where $\lambda_B = 358_{-30}^{+38}(343_{-20}^{+22})$ MeV is obtained by comparing the $B \rightarrow \pi(\rho)$ form factor from LCSR with pion [73] (rho [8]) and B meson DAs.

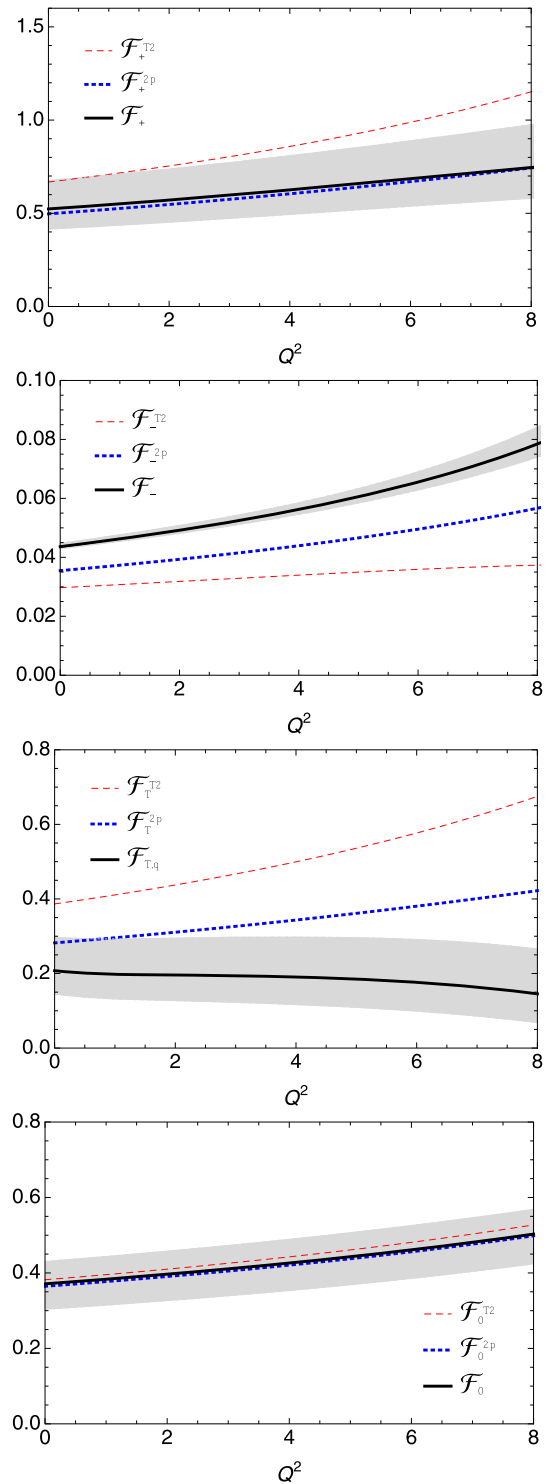


Fig. 1 LCSR predictions for $\bar{B}_s \rightarrow f_0$ form factors with $Q^2 = q^2$, where the red-dashed and blue-dotted curves represent the contributions with considering only the leading twist and also the high twists two-particle DAs of \bar{B}_s meson, respectively. The black curves indicate the form factors obtained with including both two- and three-particle DAs

Table 1 $\bar{B}_s \rightarrow f_0(980)$ form factors at $q^2 = 0$ ($q^2 = 4m_\pi^2$ for [75]) predicted in different methods

Methods	\mathcal{F}_+	\mathcal{F}_-	\mathcal{F}_T
PQCD [74]	0.70	$\equiv 0$	0.40
CLFD [75]	0.80	$\equiv 0$	–
CQM [76]	0.254	–	0.285
QCDSRs [33]	0.12	–0.07	–0.08
LCSRs [34]	0.37	$\equiv 0$	0.228
LCSRs – chiral [35]	0.44	–0.44	0.58
LCSRs [36]	0.90	0.14	0.60
This work	0.52	0.04	0.21

4 The width effect and the $\bar{B}_s \rightarrow KK$ form factors

To investigate the width effect of intermediate states, let’s look back to the dispersion relation of correlation function in Eq. 15,

$$\Pi_v(p, q) = \frac{1}{\pi} \int_0^\infty ds \frac{\text{Im}\Pi_v(s, q^2)}{s - p^2 - i\epsilon}. \tag{33}$$

The imaginary part in the numerator, corresponding to the physical regions ($q^2 > 0$), can be obtained by interpolating a complete set of intermediate states between two local currents in the correlation function,

$$2 \text{Im}\Pi_v(s, q^2) = \sum_n \int d\tau_n (2\pi)^4 \delta(s - p_n^2) \cdot \langle 0 | J^s | S_n(p) \rangle \langle S_n(p) | J_v^\dagger(q^2) | \bar{B}_s(q + p_n) \rangle, \tag{34}$$

where p and $d\tau_n$ denote the momentum and phase space volume of each state $|S_n\rangle$, respectively. In the narrow width approximation, $|S_n\rangle$ are single mesons and the dispersion relation reduces to

$$\begin{aligned} \Pi_v(p^2, q^2) &= \frac{m_{f_0} \bar{f}_{f_0} \langle f_0(p) | J_v^\dagger(q) | \bar{B}_s(p + q) \rangle}{m_{f_0}^2 - p^2 - i\epsilon} \\ &+ \frac{1}{\pi} \int_{s_0}^\infty ds \frac{\text{Im}\Pi_v(s, q^2)}{s - p^2 - i\epsilon}. \end{aligned} \tag{35}$$

In Eq. 35, only the contribution from ground state is singled out while the rest parts are retained in the integral, this is exactly what we did in the last section.

A straightforward way to consider the width effect is to substitute the interpolation of single mesons by stable multi-meson states, such as the KK , $\pi\pi$, $\eta\eta$ and their continuum states [12],

$$\begin{aligned} \Pi_v(k^2, q^2) &= \frac{1}{\pi} \int_{4m_K^2}^{s_0^{2K}} ds \int d\tau_{2K} \\ &\cdot \frac{\langle 0 | J^s | KK_{I=0} \rangle \langle KK_{I=0} | J_v^\dagger(q) | \bar{B}_s(k + q) \rangle}{s - k^2 - i\epsilon} + \dots \end{aligned} \tag{36}$$

Here we only write out explicitly the term contributed from KK state, the ellipsis denotes the contributions from $\pi\pi$, 4π , $\eta\eta$, $\eta\eta'$ and their excited states. Because it is much more harder to generate a $\bar{s}s$ pair than a $\bar{n}n$ pair from vacuum, the contribution from $\eta\eta$, $\eta\eta'$ channels can be expected to be small. The contributions from $\pi\pi$ and 4π channels are also small since they are produced via $KK \rightarrow \pi\pi, 4\pi$ rescattering, which exceeds the scope we are discussing here. In the follow calculation we consider KK state as the ground state which gives dominant contribution to the correlation function, while the contributions from high excited multi-meson states are suppressed by the Borel exponent e^{-s/M^2} (with the Borel mass $M^2 \lesssim 1.1 \text{ GeV}^2$).

4.1 Formalism

The scalar isoscalar kaon form factor is defined as [77]

$$\langle K^\rho(k_1) K^\sigma(k_2)_{I=0} | J^s | 0 \rangle = \frac{\Gamma_K^s(k^2)}{m_s} \delta^{\rho\sigma}. \tag{37}$$

There is no experiment measurement for Γ_K^s as yet,⁵ so our calculation relies on the theoretical input. In the chiral perturbative theory (CHPT), Γ_K^s has been derived to next-to-leading-order [84] with supplementing by the unitarity constraint [85], however, the unitarized CHPT works only at low energies, say, $s < 1.1 \text{ GeV}^2$ [86,87]. In order to include the high energy behaviour, one is forced to employ a model [88,89] and/or to adopt the perturbative QCD approximation [90].

From the view of hadron, Γ_K^s is relevant to the T matrix elements of $\pi\pi \rightarrow KK$ and $KK \rightarrow KK$ scatterings [88,89] via

$$\Gamma_K^s(k^2) = M_K(k^2) + T_{Ki} G_{ii} M_i, \tag{38}$$

⁵ For the scalar isoscalar pion form factor Γ_π defined with $\bar{n}n$ source current, the N -subtracted omnés representation gives a good description for the data up to $k^2 = 1.5^2 \text{ GeV}^2$ with considering the generalized Watson theorem of the $\pi\pi \rightarrow \pi\pi$ phase [78–83].

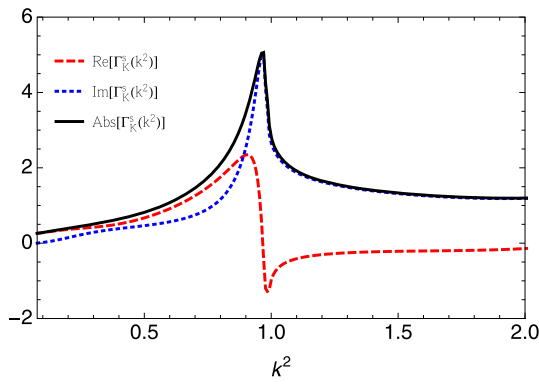


Fig. 2 The moduli of Γ_K^s obtained from $I = J = 0$ hadronic $KK \rightarrow KK$ scattering

where M_i , in principle, is an analytic term describing the transition from the scalar isoscalar source to the channel i ($i = 1$ represents for $\pi\pi$ and $i = 2$ for KK), and G_{ii} is the free propagation of the particles in channel i . The $\pi\pi$ channel does not contribute to the $\bar{s}\Gamma_v^T b$ transition at Born level, which is one of the reasons we can obtain the approximate dispersion relation in Eq. 36, with retaining only the KK channel. To maintain the self-consistency of the interpolation, we take only the KK channel in Eq. 38 too, and the transition from source current J^s to KK channel happens as $G_{KK}M_K = 1$ with subsequently the free propagating. In this way, a simple relation is obtained as

$$\Gamma_K^s(k^2) = M_K(0) + T_{KK}(k^2), \tag{39}$$

with the normalisation $M_K(0) = m_K^2 - m_\pi^2/2$.

We can read from Eqs. (38, 39) that the phase of s flavoured kaon form factor is only determined by the $KK \rightarrow KK$ scattering amplitude, whose expression with definite isospin (I) and partial wave (J) is parameterised as

$$\begin{aligned} T_J^I(k^2) &= \frac{1}{2i\beta_K(k^2)} \left[\eta_J^I(k^2) e^{2i\delta_J^I(k^2)} - 1 \right] \\ &= |T_J^I(k^2)| e^{i\phi_J^I(k^2)}. \end{aligned} \tag{40}$$

In the above equation, $\beta_K(k^2) = \sqrt{1 - 4m_K^2/k^2}$ is the phase space of KK system, η_J^I and δ_J^I are the inelasticity and phase shift, respectively, and ϕ_J^I is the phase. We would use the result of $T_0^0(k^2)$ obtained from the amplitude analysis [91, 92] as input for the scalar form factor,⁶ which, as they claimed, can be extrapolated to a high energy $\sim 5 \text{ GeV}^2$. We show in Fig. 2 for the result in the energy regions $k^2 \in [4m_\pi^2, 2.0] \text{ GeV}^2$, these curves consist with the result obtained from CHPT in the low energy regions $k^2 < 1.1 \text{ GeV}^2$ [86], and also consist with the fully K -matrix description in the high energies [89]. The amplitude analysis result we adopted here

⁶ We thanks Ling-yun Dai for sharing us with the original result of their global fit analysis.

considered all the measured data, the $\pi\pi - K\bar{K}$ final state interaction, the mass difference between the charged and neutral kaon, and the low energy Roy equation [93]. In the amplitude analysis demonstrated by coupled-channel treatment and combined fitting, the source current with $s\bar{s}$ configuration is overwhelming coupled to KK channel through f_0 , while the coupling to $\pi\pi$ is tiny.

The remaining matrix element in Eq. 36 are defined in terms of $\bar{B}_s \rightarrow KK$ transition form factors [94], for the axial-vector current j_v^A we have

$$\begin{aligned} &-i \langle K^+(k_1) K^-(k_2) | \bar{s} \gamma_\nu \gamma_5 b | \bar{B}_s(q+k) \rangle \\ &= F_t \frac{q_\nu}{\sqrt{q^2}} + F_0 \frac{2\sqrt{q^2}}{\sqrt{\lambda_B}} \left(k_\nu - \frac{k \cdot q}{q^2} q_\nu \right) \\ &+ \frac{F_\parallel}{\sqrt{k^2}} \left(\bar{k}_\nu - \frac{4(q \cdot k)(q \cdot \bar{k})}{\lambda_B} k_\nu + \frac{4k^2(q \cdot \bar{k})}{\lambda_B} q_\nu \right). \end{aligned} \tag{41}$$

The kinematics of \bar{B}_s decay to KK state are described by three independent variables: k^2 , q^2 and θ_K , denoting the invariant mass of KK system, the squared momentum transfer in the weak decay and the angle between the 3 momentum of $K^-(k_2)$ and \bar{B}_s meson in the K^+K^- rest frame, respectively. The dot products are

$$\begin{aligned} q \cdot k &= \frac{1}{2}(m_{B_s}^2 - k^2 - q^2), \\ q \cdot \bar{k} &= \frac{\sqrt{\lambda_B}}{2} \beta_K(k^2) \cos \theta_K, \end{aligned} \tag{42}$$

with the kinematic Källén function $\lambda_B \equiv \lambda(m_{B_s}^2, q^2, k^2) = m_{B_s}^4 + k^4 + q^4 - 2(m_{B_s}^2 k^2 + m_{B_s}^2 q^2 + k^2 q^2)$. By the way, the matrix element in Eq. 41 can also be defined by the helicity amplitudes,

$$H_\lambda = \langle K^+(k_1) K^-(k_2) | \bar{s} \gamma_\nu \gamma_5 b | \bar{B}_s(q+k) \rangle. \tag{43}$$

The helicity definition provides a possibility to study the contributions from different partial waves, because H_λ , with $\lambda = t, 0, +, -$, can be expanded in terms of the associated Legendre polynomials. To study the partial waves contributions within the convenient definition in orthogonal Lorentz structures, we translate the partial wave expansion from the helicity amplitudes H_λ to the form factors F_i ,

$$\begin{aligned} &F_{0,t}(q^2, k^2, q \cdot \bar{k}) \\ &= \sum_{l=0}^{\infty} \sqrt{2l+1} F_{0,t}^{(l)}(q^2, k^2) P_l^{(0)}(\cos \theta_\pi), \\ &F_\parallel(q^2, k^2, q \cdot \bar{k}) \\ &= \sum_{l=1}^{\infty} \sqrt{2l+1} F_\parallel^{(l)}(q^2, k^2) \frac{P_l^{(1)}(\cos \theta_\pi)}{\sin \theta_\pi}. \end{aligned} \tag{44}$$

Considering the decomposition of isoscalar KK state,

$$|KK_{I=0}\rangle = \frac{1}{\sqrt{2}}|K^+K^-\rangle + \frac{1}{\sqrt{2}}|K^0\bar{K}^0\rangle, \tag{45}$$

substituting Eqs. 41 and 44 into Eq. 36, we obtain the S -wave contribution to the imaginary part with interpolating scalar isoscalar KK state,

$$\begin{aligned} & \int d\tau_{2K} \langle 0|J^S|KK_{I=0}\rangle \langle KK_{I=0}|J_v^A(q)|\bar{B}_s(k+q)\rangle \\ &= \int d\tau_{2K} 2 \frac{\Gamma_K^{S*}(k^2)}{m_s} \langle K^+(k_1)K^-(k_2)|J_v^A(q)|\bar{B}_s(p+k)\rangle \\ &= 2i \frac{\beta_K(s)}{8\pi} \frac{\Gamma_K^{S*}(s)}{m_s} \left[F_0^{(l=0)}(q^2, s) \frac{2\sqrt{q^2}}{\sqrt{\lambda_B}} k_v \right. \\ & \quad \left. + \left(\frac{F_t^{(l=0)}(q^2, k^2)}{\sqrt{q^2}} - F_0^{(l=0)}(q^2, s) \frac{2\sqrt{q^2}}{\sqrt{\lambda_B}} \frac{k \cdot q}{q^2} \right) q_v \right]. \end{aligned} \tag{46}$$

In fact, the phase space $d\tau_{2K}$ plays as a S -wave projector for the timelike-helicity form factors $F_{t,0}$, which means that only the S -wave component $F_{t,0}^{(l=0)}$ survives after integrating over the angle θ_K . For the form factor F_{\parallel} , the role of S -wave projector vanishes and the contribution starts from D -wave component ($l = 2n, n = 1, 2, 3 \dots$), which part is expected tiny in the $\bar{B}_s \rightarrow KK$ transition and would not be discussed in this paper.

We take the global duality to eliminate the contributions beyond KK state with the threshold s_0^{2K} ,

$$\begin{aligned} & \frac{1}{\pi} \int_{s_0^{2K}}^{\infty} ds e^{-s/M^2} \mathbf{Im} \Pi_v(s, q^2) \\ &= \frac{1}{\pi} \int_{s_0^{2K}}^{\infty} ds e^{-s_q/M^2} \mathbf{Im} \Pi_v^{\text{OPE}}(s_q, q^2), \end{aligned} \tag{47}$$

and arrive at the LCSRs result for S -wave $\bar{B}_s \rightarrow KK$ transition,

$$\begin{aligned} & \int_{4m_K^2}^{s_0^{2K}} ds e^{-s/M^2} \frac{\beta_K(s)}{4\pi^2} \frac{\Gamma_K^{S*}(s)}{m_s} F_0^{(l=0)}(q^2, s) \frac{\sqrt{q^2}}{\sqrt{\lambda_B}} \\ &= f_{B_s} m_{B_s}^2 \left\{ \int_0^{\sigma_0^{2K}} d\sigma e^{-s_q/M^2} \left[\phi_+(\sigma m_{B_s}) \right. \right. \\ & \quad \left. \left. - \frac{\bar{\phi}_{\pm}(\sigma m_{B_s})}{\bar{\sigma} m_{B_s}} - \frac{8\bar{\sigma} m_{B_s}^2 g_+(\sigma m_{B_s})}{(\bar{\sigma}^2 m_{B_s}^2 - q^2)^2} \right. \right. \\ & \quad \left. \left. - \frac{4\bar{\sigma} g'_+(\sigma m_{B_s})}{(\bar{\sigma}^2 m_{B_s}^2 - q^2)} \right] + \Delta\mathcal{F}_+(q^2, s_0^{2K}, M^2) \right\}, \tag{48} \\ & \int_{4m_K^2}^{s_0^{2K}} ds e^{-s/M^2} \frac{\beta_{\pi}(s)}{8\pi^2} \frac{\Gamma_K^{S*}(s)}{m_s} \\ & \cdot \left(\frac{F_t^{(l=0)}(q^2, k^2)}{\sqrt{q^2}} - F_0^{(l=0)}(q^2, s) \frac{2\sqrt{q^2}}{\sqrt{\lambda_B}} \frac{k \cdot q}{q^2} \right) \end{aligned}$$

$$\begin{aligned} &= f_{B_s} m_{B_s}^2 \left\{ \int_0^{\sigma_0^{2K}} d\sigma e^{-s_q/M^2} \left[-\frac{\sigma}{\bar{\sigma}} \phi_+(\sigma m_{B_s}) \right. \right. \\ & \quad \left. \left. - \frac{\bar{\phi}_{\pm}(\sigma m_{B_s})}{\bar{\sigma} m_{B_s}} + \frac{8\bar{\sigma} \sigma m_{B_s}^2 g_+(\sigma m_{B_s})}{(\bar{\sigma}^2 m_{B_s}^2 - q^2)^2} \right. \right. \\ & \quad \left. \left. + \frac{4\sigma g'_+(\sigma m_{B_s})}{(\bar{\sigma}^2 m_{B_s}^2 - q^2)} \right] + \Delta\mathcal{F}_-(q^2, s_0^{2K}, M^2) \right\}, \end{aligned} \tag{49}$$

Multiplying both sides of Eq. 46 by q^v , we obtain another independent LCSRs for the timelike-helicity form factor $F_t^{(l=0)}(q^2, s)$,

$$\begin{aligned} & \int_{4m_K^2}^{s_0^{2K}} ds e^{-s/M^2} \frac{\beta_{\pi}(s)}{8\pi^2} \frac{\Gamma_K^{S*}(s)}{m_s} \sqrt{q^2} F_t^{(l=0)}(q^2, s) \\ &= f_{B_s} m_{B_s}^2 m_b \left\{ \int_0^{\sigma_0^{2K}} d\sigma e^{-s_q/M^2} \right. \\ & \cdot \left[\frac{(\bar{\sigma}^2 m_{B_s}^2 - q^2) \phi_+(\sigma m_{B_s})}{2\bar{\sigma}^2 m_{B_s}} - \frac{3\bar{\phi}_{\pm}(\sigma m_{B_s})}{\bar{\sigma}} \right. \\ & \quad \left. - \left[2\bar{\sigma} m_{f_0}^2 - 2\sigma q^2 + (1 - 2\sigma)(m_{B_s}^2 - m_{f_0}^2 - q^2) \right] \right. \\ & \quad \left. \cdot \left(\frac{\bar{\sigma} m_{B_s} g_+(\sigma m_{B_s})}{(\bar{\sigma}^2 m_{B_s}^2 - q^2)^2} + \frac{g'_+(\sigma m_{B_s})}{2m_{B_s}(\bar{\sigma}^2 m_{B_s}^2 - q^2)} \right) \right] \\ & \quad \left. + \Delta\mathcal{F}_0(q^2, s_0^{2K}, M^2) \right\}. \end{aligned} \tag{50}$$

4.2 Models

Equations (48, 49, 50) are the main results in this section. Due to the convoluted integral, we can not solve out the form factors $F_{t/0}^{(l=0)}$ in terms of the B meson DAs. To propel the calculation, one way we can try is to introduce the parameterisation of S -wave $\bar{B}_s \rightarrow KK$ form factors, and the first candidate coming into our mind is the single resonance (f_0) model in the generalized Breit-Wigner formula.⁷

$$F_0^{(l=0)}(s, q^2) \frac{\sqrt{q^2}}{\sqrt{\lambda_B}} = \frac{1}{\sqrt{2}} \frac{g_{f_0 KK} \mathcal{F}_+^{\bar{B}_s \rightarrow f_0}(q^2)}{m_{f_0}^2 - s - i\sqrt{s} \Gamma_{f_0}(s)} e^{i\phi_{f_0}(s, q^2)}, \tag{51}$$

$$\begin{aligned} & \frac{1}{\sqrt{2}} \left(\frac{F_t^{(l=0)}(s, q^2)}{\sqrt{q^2}} - F_0^{(l=0)}(s, q^2) \frac{\sqrt{q^2}}{\sqrt{\lambda_B}} \frac{m_{B_s}^2 - s - q^2}{q^2} \right) \\ &= \frac{g_{f_0 KK} \mathcal{F}_-^{\bar{B}_s \rightarrow f_0}(q^2)}{m_{f_0}^2 - s - i\sqrt{s} \Gamma_{f_0}(s)} e^{i\phi_{f_0}(s, q^2)}, \tag{52} \\ & \frac{1}{\sqrt{2}} F_t^{(l=0)}(s, q^2) \sqrt{q^2} \end{aligned}$$

⁷ We drop the σ with the same reasons as described in Sect. 3, which, phenomenologically, is further supported by the fact that no any signal is found for KK coupling to σ [50].

$$= \frac{g_{f_0 KK} \mathcal{F}_0^{\bar{B}_s \rightarrow f_0}(q^2)(m_{\bar{B}_s}^2 - m_{f_0}^2)}{m_{f_0}^2 - s - i\sqrt{s} \Gamma_{f_0}(s)} e^{i\phi_{f_0}(s,q^2)}, \tag{53}$$

The strong coupling $g_{f_0\pi\pi}$ is normalized as

$$\langle K^+(k_1)K^-(k_2)|f_0^s(k_1+k_2)\rangle = g_{f_0 K^+ K^-} = \frac{g_{f_0 KK}}{\sqrt{2}}. \tag{54}$$

An underlying condition implied in Eqs. (48, 49, 50) is the reality of expressions on the left hand side, and we take the more strict local reality at each point of invariant mass,

$$\text{Im}\left[\Gamma_{\bar{K}}^{s*}(s)F_{0/t}^{(l=0)}(q^2, s)\right] = 0. \tag{55}$$

To fulfil this requirement, a strong phase ϕ_{f_0} is introduced to compensate the phase difference between the kaon form factor and the modeled $\bar{B}_s \rightarrow KK$ form factors. Generally speaking, ϕ_{f_0} should depend on both the two variables s and q^2 , while in the single f_0 model the q^2 -dependence disappears,

$$\delta\Gamma_{\bar{K}}^s(s) - \phi_{f_0}(s) = \text{Arg}\left[\frac{g_{f_0 KK}}{m_{f_0}^2 - s - i\sqrt{s}\Gamma_{f_0}(s)}\right]. \tag{56}$$

The simple model in Eqs. (51–53) is inspired by the physics that the sum rules obtained for the $\bar{B}_s \rightarrow KK$ form factors, in the narrow width approximation, should reproduce the sum rules for the form factors of $\bar{B}_s \rightarrow f_0$ transition. To check this, let’s consider the energy-dependent width of f_0 with including the loop effects of two kaons coupling,

$$\begin{aligned} \Gamma_{f_0}(s) &= \frac{g_{f_0 KK}^2 \beta_K(s)}{4\sqrt{2}\pi\sqrt{s}} \Theta(s - 4m_K^2) \\ &= \Gamma_{f_0}^{\text{tot}} \frac{\beta_K(s)}{\beta_K(m_{f_0})} \frac{m_{f_0}}{\sqrt{s}} \Theta(s - 4m_K^2). \end{aligned} \tag{57}$$

The width of f_0 is usually parameterized under the Flatté model [95,96] with considering the location of f_0 in the invariant mass, say, below or above the threshold. While in the \bar{B}_s decays, the case is different because the invariant mass is always above the threshold,⁸ then we can take the conventional form of the width as described in Eq. 57. In the single f_0 model, the s flavoured kaon form factor is written as

$$\left.\frac{\Gamma_{\bar{K}}^{s*}(s)}{m_s}\right|_{f_0} = \frac{g_{f_0 KK} m_{f_0} \bar{f}_{f_0}^s}{m_{f_0}^2 - s + i\sqrt{s}\Gamma_{f_0}(s)} e^{-i\phi_{f_0}(s,q^2)}. \tag{58}$$

Substituting Eqs. (51, 58) into Eq. 48, the left hand side of Eq. 48 becomes

$$m_{f_0} \bar{f}_{f_0} \mathcal{F}_+^{\bar{B}_s \rightarrow f_0}(q^2) \int_{4m_K^2}^{s_0^{2K}} ds e^{-s/M^2} \frac{1}{\pi} \frac{\Gamma_{f_0}(s)\sqrt{s}}{(m_{f_0}^2 - s)^2 + s\Gamma_{f_0}^2(s)}$$

⁸ Another reason for us not using the Flatté model is that it gives a smaller value of $I^{f_0} = 4.44_{-0.98}^{+0.81}$, which is close to $I^{f_0'}$ and damages the contribution hierarchy from different resonances, as we would see in Eqs. (68, 69).

$$\xrightarrow{\Gamma_{f_0}^{\text{tot}} \rightarrow 0} m_{f_0} \bar{f}_{f_0} \mathcal{F}_+^{\bar{B}_s \rightarrow f_0}(q^2) e^{-m_{f_0}^2/M^2}. \tag{59}$$

Similarly, we can reproduce the LCSRs for form factors $\mathcal{F}_-^{\bar{B}_s \rightarrow f_0}$ and $\mathcal{F}_0^{\bar{B}_s \rightarrow f_0}$ with taking into account the resonance models in Eqs. 52 and 53, respectively. What’s more, the relation defined in Eq. 23 also holds in the resonance models.

4.3 Numerics

We employ the z -series expansion for heavy-to-light transition form factors [97], with $j = +, -, 0$,

$$\mathcal{F}_j^{\bar{B}_s \rightarrow f_0}(q^2) = \frac{\mathcal{F}_j^{\bar{B}_s \rightarrow f_0}(0)}{1 - q^2/m_{B_s}^2} \left\{ 1 + b_{\mathcal{F}_j} \zeta(q^2) + c_{\mathcal{F}_j} \zeta^2(q^2) \right\}. \tag{60}$$

$\mathcal{F}_j^{\bar{B}_s \rightarrow f_0}(0)$ is the value at the full recoiled energy, the parameters $b_{\mathcal{F}_j}, c_{\mathcal{F}_j}$ indicate the coefficients associated with the ζ -functions,

$$\zeta(q^2) = z(q^2) - z(0), \tag{61}$$

$$z(q^2) = \frac{\sqrt{t_+ - q^2} - \sqrt{t_+ - t_0}}{\sqrt{t_+ - q^2} + \sqrt{t_+ - t_0}}, \tag{62}$$

with the definitions $t_{\pm} \equiv (m_{B_s} \pm m_{f_0})^2$ and $t_0 \equiv t_+(1 - \sqrt{1 - t_-/t_0})$.

The S -wave $\bar{B}_s \rightarrow KK$ form factors, under the single f_0 model, is rearranged in a general formula as

$$\begin{aligned} &\left[X_{\mathcal{F}_j} I(s_0^{2K}, M^2, \Gamma_{f_0}^{\text{tot}})\right] \frac{\kappa_{\mathcal{F}_j} + \eta_{\mathcal{F}_j} \zeta(q^2) + \rho_{\mathcal{F}_j} \zeta^2(q^2)}{1 - q^2/m_{B_s}^2} \\ &= I_j^{\text{OPE}}(s_0^{2K}, M^2, q^2), \end{aligned} \tag{63}$$

where for the sake of brevity we introduce the following notations:

$$\begin{aligned} \kappa_{\mathcal{F}_j} &\equiv |g_{f_0 KK}| \mathcal{F}_j^{\bar{B}_s \rightarrow f_0}(0), \\ \eta_{\mathcal{F}_j} &\equiv b_{\mathcal{F}_j} |g_{f_0 KK}| \mathcal{F}_j^{\bar{B}_s \rightarrow f_0}(0), \\ \rho_{\mathcal{F}_j} &\equiv c_{\mathcal{F}_j} |g_{f_0 KK}| \mathcal{F}_j^{\bar{B}_s \rightarrow f_0}(0), \\ X_{\mathcal{F}_+} &= X_{\mathcal{F}_-} = 1, \quad X_{\mathcal{F}_0} = (m_{B_s}^2 - m_{f_0}^2). \end{aligned} \tag{64}$$

The integral coefficient on the left hand side reads as

$$\begin{aligned} &I(s_0^{2K}, M^2, \Gamma_{f_0}^{\text{tot}}) \\ &= \frac{1}{4\sqrt{2}\pi^2} \int_{4m_K^2}^{s_0^{2K}} ds e^{-s/M^2} \frac{\beta_K(s) |\Gamma_{\bar{K}}^s(s)/m_s|}{\sqrt{(m_{f_0}^2 - s)^2 + s\Gamma_{f_0}^2(s)}}. \end{aligned} \tag{65}$$

I_j^{OPE} represents the OPE calculations on the right hand side of Eqs. (48, 49, 50). There is no physical requirement that the threshold value s_0^{2K} should be equal to s_0 , we fixed it in an independent way by considering the correlation function

in Eq. 1 with KK interpolating. The 2pSRs is then written in terms of the scalar isoscalar kaon form factor,

$$\int_{4m_K^2}^{s_0^{2K}} ds e^{-s/M^2} \frac{\beta_K(s)}{8\pi^2} \left| \frac{\Gamma_K^S(s)}{m_s} \right|^2 = \Pi_{2pSRs}^{OPE}(s_0^{2\pi}, M^2). \tag{66}$$

We then determine the value $s_0^{2K} = 2.0 \text{ GeV}^2$, closing to it taken in the case of single meson interpolating.

Besides the bound state f_0 , it is nature to question what’s the roles of the excited states f_0', f_0'' in the $\bar{B}_s \rightarrow KK$ transition.⁹ To include these effects, we suggest the $f_0 + f_0' + f_0''$ model by appending f_0' and f_0'' states to Eq. (53),

$$\begin{aligned} & \frac{1}{\sqrt{2}} F_t^{(l=0)}(s, q^2) \sqrt{q^2} \\ &= \sum_{S=f_0, f_0', f_0''} \frac{g_{SKK} \mathcal{F}_0^{\bar{B}_s \rightarrow S}(q^2) (m_{B_s}^2 - m_S^2)}{m_S^2 - s - i\sqrt{s}\Gamma_S(s)} e^{i\phi_S(s)}. \end{aligned} \tag{67}$$

We tacitly assume that the strong phase ϕ_S associated to each intermediate state is only dependent on the invariant mass of dikaon state, which means we do not consider the interaction effect between different resonances when introducing the strong phases to satisfy Eq. 55. By this way, the $\bar{B}_s \rightarrow S$ form factors for different intermediate resonances are linear to each other: $\mathcal{F}_j^{f_0'}(q^2) = \gamma_{\mathcal{F}_j}^{f_0'} \mathcal{F}_j^{f_0}(q^2)$ and $\mathcal{F}_j^{f_0''}(q^2) = \gamma_{\mathcal{F}_j}^{f_0''} \mathcal{F}_j^{f_0}(q^2)$. The dimensionless parameters $\gamma_{\mathcal{F}_j}^{f_0'}$ and $\gamma_{\mathcal{F}_j}^{f_0''}$ indicate the relative size of $\bar{B}_s \rightarrow f_0'$ and f_0'' form factors comparing to the $\bar{B}_s \rightarrow f_0$ form factors, respectively. The LCSRs in Eq. 63, in the case of three resonance model, is modified to

$$\begin{aligned} & \sum_{S=f_0, f_0', f_0''} \left[\gamma_{\mathcal{F}_j}^S X_{\mathcal{F}_j}^S I^S \right] \frac{\kappa_{\mathcal{F}_j} + \eta_{\mathcal{F}_j} \zeta(q^2) + \rho_{\mathcal{F}_j} \zeta^2(q^2)}{1 - q^2/m_{B_s}^2} \\ &= I_j^{OPE}(s_0^{2K}, M^2, q^2). \end{aligned} \tag{68}$$

We quote the values of the integral coefficients (in unit of 10^{-2})

$$I^{f_0} = 9.54_{-1.54}^{+1.48}, \quad I^{f_0'} = 3.67_{-1.38}^{+2.30}, \quad I^{f_0''} = 1.82_{-0.57}^{+0.73}. \tag{69}$$

In these integrals with taking the bound limit at $4m_K^2$, only the right half of the peaking region in Fig. 2 is taken into account, so the relative sizes of integral coefficients $I^{f_0'}, I^{f_0''}$ to I^{f_0} ($I^{f_0'}/I^{f_0}, I^{f_0''}/I^{f_0}$) can be expected to be double of that in the $B \rightarrow \pi\pi$ case [12].

The fitting result in the $f_0 + f_0' + f_0''$ model are presented in Table 2, where the errors come from the sum rules

⁹ Hereafter we take f_0, f_0' and f_0'' to denote the meson states $f_0(980), f_0(1500)$ and $f_0(1710)$, respectively. We do not consider $f_0(1370)$ as a separated resonance due to the weak coupling of $f_0(1370)$ to KK state.

Table 2 The fitting result for \mathcal{F}_i in $f_0 + f_0' + f_0''$ model

$ g_{S\pi\pi} _{\mathcal{F}_j}$	$ g_{S\pi\pi} _{\mathcal{F}_+}$	$ g_{S\pi\pi} _{\mathcal{F}_0}$
$\kappa_{\mathcal{F}_j}^{f_0}$ (GeV)	$0.56_{-0.08}^{+0.02}$	$0.40_{-0.05}^{+0.01}$
$\eta_{\mathcal{F}_j}^{f_0}$ (GeV)	$-0.97_{+0.13}^{-0.01}$	$0.19_{-0.19}^{+0.15}$
$\rho_{\mathcal{F}_j}^{f_0}$ (GeV)	$-12.5_{-1.42}^{+2.60}$	$0.61_{+0.57}^{-0.60}$
$\gamma_{\mathcal{F}_j}^{f_0'}$	$0.49_{-0.17}^{+0.45}$	$0.48_{-0.16}^{+0.26}$
$\gamma_{\mathcal{F}_j}^{f_0''}$	$0.66_{-0.20}^{+0.80}$	$0.62_{-0.26}^{+0.58}$
$\mathcal{F}_+^{\bar{B}_s \rightarrow f_0}(0)$	0.52 ± 0.10	$\mathcal{F}_0^{\bar{B}_s \rightarrow f_0}(0)$
		0.37 ± 0.06

parameters. For the total widths of the intermediate resonances we choose $\Gamma_{f_0}^{\text{tot}} = 0.055 \text{ GeV}$, $\Gamma_{f_0'}^{\text{tot}} = 0.112 \text{ GeV}$ and $\Gamma_{f_0''}^{\text{tot}} = 0.123 \text{ GeV}$ [50]. We note that varying the width of f_0 in $[0.01, 0.1] \text{ GeV}$ brings another uncertainty to I^{f_0} by ${}_{-1.40}^{+2.55}$, while the width effects of f' (f'') to I^{f_0} ($I^{f_0''}$) is negligible since their widths are much smaller. In the fit we also use the condition at $q^2 = 0$

$$\sum_{S=f_0, f_0', f_0''} \left[\gamma_{\mathcal{F}_j}^S X_{\mathcal{F}_j}^S I^S \right] \kappa_{\mathcal{F}_j} = I_j^{OPE}(s_0^{2K}, M^2, 0), \tag{70}$$

and also the hierarchy anstz of different resonances in the left hand side of Eq. 68, say, $0 < \gamma_{\mathcal{F}_j}^{f_0'}, \gamma_{\mathcal{F}_j}^{f_0''} < 1$. At the bottom of Table 2, for the comparison we supplement the $\bar{B}_s \rightarrow f_0$ form factors calculated in Sect. 3 under the narrow width approximation. In principle, the strong coupling $|g_{f_0KK}|$ can be extracted out in case we have the reliable prediction for $\bar{B}_s \rightarrow f_0$ form factors, \mathcal{F}_+ and \mathcal{F}_0 . With the result obtained in the narrow width approximation as we demonstrated in the last section, we can estimate $|g_{f_0KK}| = 1.08_{-0.14}^{+0.05} \text{ GeV}$, but keep in mind that the width/non-resonant effect is sizeable and we reserve another $\sim 50\%$ uncertainty.

The contribution from each resonance to the OPE result (Eq. 68) is listplotted in Fig. 3, from which the expected leading role of f_0 is confirmed. We plot in Fig. 4 for the S -wave $\bar{B}_s \rightarrow KK$ form factors in the $f_0 + f_0' + f_0''$ model, for convenience we also show the part of contributions from f_0 in blue dashed curves. It is easy to see the overwhelming role of f_0 , while the contributions from f_0' and f_0'' account only $\sim 5\%$. The result at the full recoiled energy $\sqrt{q^2} F_t^{(l=0)}(1, 0)/m_{B_s} = 54.0_{-7.0}^{+4.0}$ is much larger than the result for S -wave $B \rightarrow \pi\pi$ form factors obtained in the LCSRs with 2π DAs [98–100], with the asymptotic prediction $\sqrt{q^2} F_t^{(l=0)}(4m_\pi^2, 0)/m_B = 5.40 \pm 1.00$, this discrepancy is explained by the strong threshold effect of f_0 in the $\bar{B}_s \rightarrow KK$ decay.

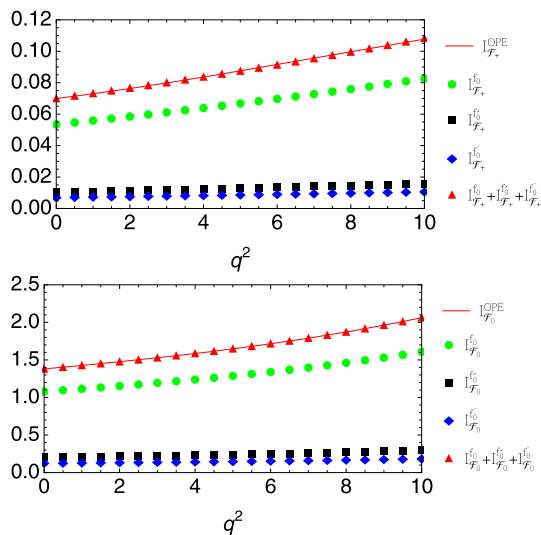


Fig. 3 The contributions to the OPE result $I_{\mathcal{F}_+}^{\text{OPE}}$ (up) and $I_{\mathcal{F}_0}^{\text{OPE}}$ (down) in the $f_0 + f'_0 + f''_0$ model

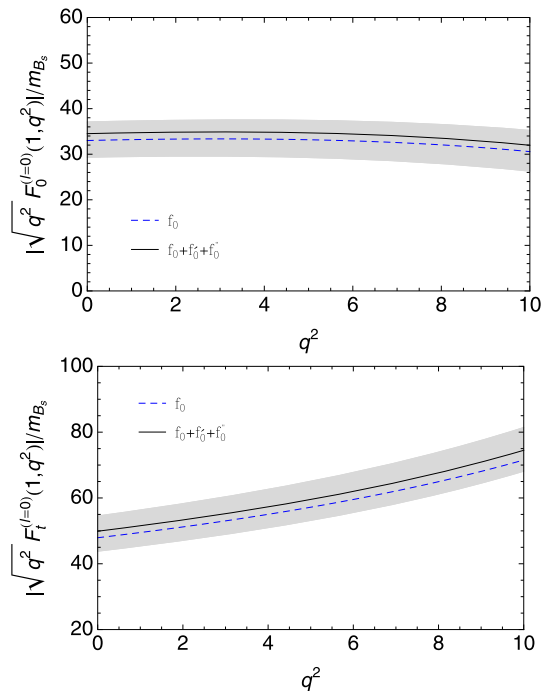


Fig. 4 $\sqrt{q^2} F_0^{(l=0)}(1, q^2)/m_{B_s}$ and $\sqrt{q^2} F_t^{(l=0)}(1, q^2)/m_{B_s}$ obtained under the $f_0 + f'_0 + f''_0$ model

5 Conclusion

In this paper we calculate the $\bar{B}_s \rightarrow f_0(980)$ form factor from the light-cone sum rules with B -meson DAs, and investigate the S -wave $\bar{B}_s \rightarrow KK$ form factors to study the width effect, basing on the assumption that f_0 is dominated by the $\bar{s}s$ configuration. With taking the conventional quark-antiquark assignment, we revisit the 2pSRs for the mass and decay constant of $f_0(980)$. For the $\bar{B}_s \rightarrow f_0(980)$

form factors, we find that the high twist two-particle and the three-particle B -meson DAs give 25% correction separately, and their total correction to certain form factors can be about 50%. In order to investigate the width effect, we suggest the three resonance states model to parameterize the S -wave $\bar{B}_s \rightarrow KK$ form factors, the fitting result shows the dominant role of f_0 , and as a by-product, suggest a new way to determine the strong coupling $|g_{f_0 KK}|$. The residual uncertainty of our prediction mainly comes from the freedom to choose the widths of f_0 .

Acknowledgements We are grateful to Hai-yang Cheng and Ling-yun Dai for helpful discussions. This work is supported by the National Science Foundation of China under Grant Nos. 11805060 and 11905056, “the Fundamental Research Funds for the Central Universities” under Grant Nos. 531118010176 and 531118010258. S. C. is grateful to the High energy theory group at Institute of Physics, Academia Sinica for hospitality and for financial support where this work was finalized.

Data Availability Statement This manuscript has no associated data or the data will not be deposited. [Authors’ comment: Not applicable.]

Open Access This article is licensed under a Creative Commons Attribution 4.0 International License, which permits use, sharing, adaptation, distribution and reproduction in any medium or format, as long as you give appropriate credit to the original author(s) and the source, provide a link to the Creative Commons licence, and indicate if changes were made. The images or other third party material in this article are included in the article’s Creative Commons licence, unless indicated otherwise in a credit line to the material. If material is not included in the article’s Creative Commons licence and your intended use is not permitted by statutory regulation or exceeds the permitted use, you will need to obtain permission directly from the copyright holder. To view a copy of this licence, visit <http://creativecommons.org/licenses/by/4.0/>.
Funded by SCOAP³.

A B meson LCDAs

Several models have been suggested for the LCDAs with definite twists, which incorporate the correct low-momentum behaviour and satisfy the (tree-level) equation of motion (EOM) constraints [62,65,101]. In [63], a more general ansatz is proposed with comprising all of these models as particular cases.

For the two-particle B_s meson DAs demonstrated in Eq. 18, $\phi_+(\omega)$ and $\phi_-(\omega)$ are the leading and subleading twist DAs, and $g_+(\omega)$ and $g_-(\omega)$ are DAs at twist-4 and twist-5, respectively. The general model are quoted as [63]

$$\phi_+(\omega) = \omega f(\omega), \tag{71}$$

$$\phi_-(\omega) = F(\omega) - \frac{1}{6} \kappa (\lambda_E^2 - \lambda_H^2) \left[\omega^2 f'(\omega) + 4\omega f(\omega) - 2F(\omega) \right], \tag{72}$$

$$g_+(\omega) \simeq g_+^{WW}(\omega) = \frac{1}{8} \int_{\omega}^{\infty} \left[\omega^2 + 3\rho^2 - 4\bar{\lambda}\rho \right] f(\rho), \tag{73}$$

$$g_-(\omega) = -\frac{3\omega}{4}\mathcal{F}(\omega) - \frac{\omega}{4}\kappa(\lambda_E^2 - \lambda_H^2)\left[\frac{\omega^3}{3}f(\omega) + \omega F(\omega) - \mathcal{F}(\omega)\right]. \tag{74}$$

The general function $f(\omega)$ is normalized as $\int_0^\infty d\omega\omega f(\omega) = 1$ and decreases sufficiently fast at $\omega \rightarrow \infty$. In Eqs. (72, 74), three auxiliary functions are introduced to simplify the expression,

$$f'(\omega) = \frac{df(\omega)}{d\omega}, \tag{75}$$

$$F(\omega) \equiv \int_\omega^\infty d\rho f(\rho), \tag{76}$$

$$\mathcal{F}(\omega) \equiv \int_\omega^\infty d\rho_2 \int_{\rho_2}^\infty d\rho_1 f(\rho_1). \tag{77}$$

The normalization constant κ is determined from the leading twist function $f(\omega)$ via the EOM relations

$$\int_0^\infty d\omega\omega\phi_+(\omega) = \frac{4}{3}\bar{\Lambda}, \tag{78}$$

$$\int_0^\infty d\omega\omega^2\phi_+(\omega) = 2\bar{\Lambda}^2 + \frac{1}{3}(2\lambda_E^2 + \lambda_H^2), \tag{79}$$

$$\kappa^{-1} = \frac{1}{6} \int_0^\infty d\omega\omega^3\phi_+(\omega) = \bar{\Lambda}^2 + \frac{1}{6}(2\lambda_E^2 + \lambda_H^2). \tag{80}$$

Concerning the three-particle B_s meson DAs, the definitions in Eq. 19 by Lorentz structures should not be confused with the definitions by means of definite twists, and they have the following relations [62]

$$\begin{aligned} \Psi_A(\omega, \zeta) &= \frac{1}{2}[\phi_3(\omega, \zeta) + \phi_4(\omega, \zeta)], \\ \Psi_V(\omega, \zeta) &= \frac{1}{2}[-\phi_3(\omega, \zeta) + \phi_4(\omega, \zeta)], \\ X_A(\omega, \zeta) &= \frac{1}{2}[-\phi_3(\omega, \zeta) - \phi_4(\omega, \zeta) + 2\psi_4(\omega, \zeta)], \\ Y_A(\omega, \zeta) &= \frac{1}{2}[-\phi_3(\omega, \zeta) - \phi_4(\omega, \zeta) + \psi_4(\omega, \zeta) - \psi_5(\omega, \zeta)], \\ \tilde{X}_A(\omega, \zeta) &= \frac{1}{2}[-\phi_3(\omega, \zeta) + \phi_4(\omega, \zeta) - 2\tilde{\psi}_4(\omega, \zeta)], \\ \tilde{Y}_A(\omega, \zeta) &= \frac{1}{2}[-\phi_3(\omega, \zeta) + \phi_4(\omega, \zeta) - \tilde{\psi}_4(\omega, \zeta) + \tilde{\psi}_5(\omega, \zeta)], \\ W(\omega, \zeta) &= \frac{1}{2}[\phi_4(\omega, \zeta) - \psi_4(\omega, \zeta) - \tilde{\psi}_4(\omega, \zeta) \\ &\quad + \tilde{\phi}_5(\omega, \zeta) + \psi_5(\omega, \zeta) + \tilde{\psi}_5(\omega, \zeta)], \\ Z(\omega, \zeta) &= \frac{1}{4}[-\phi_3(\omega, \zeta) + \phi_4(\omega, \zeta) - 2\tilde{\psi}_4(\omega, \zeta) \\ &\quad + \tilde{\phi}_5(\omega, \zeta) + 2\tilde{\psi}_5(\omega, \zeta) - \phi_6(\omega, \zeta)]. \end{aligned} \tag{81}$$

The general model for the DAs with definite twists are [63]

$$\phi_3(\omega, \zeta) = -\frac{1}{2}\kappa(\lambda_E^2 - \lambda_H^2)\omega\zeta^2 f'(\omega + \zeta), \tag{82}$$

$$\phi_4(\omega, \zeta) = \frac{1}{2}\kappa(\lambda_E^2 + \lambda_H^2)\zeta^2 f(\omega + \zeta), \tag{83}$$

$$\psi_4(\omega, \zeta) = \kappa\lambda_E^2\omega\zeta f(\omega + \zeta), \tag{84}$$

$$\tilde{\psi}_4(\omega, \zeta) = \kappa\lambda_H^2\omega\zeta f(\omega + \zeta), \tag{85}$$

$$\tilde{\phi}_5(\omega, \zeta) = -\kappa(\lambda_E^2 + \lambda_H^2)\omega F(\omega + \zeta), \tag{86}$$

$$\psi_5(\omega, \zeta) = \kappa\lambda_E^2\zeta F(\omega + \zeta), \tag{87}$$

$$\tilde{\psi}_5(\omega, \zeta) = \kappa\lambda_H^2\zeta F(\omega + \zeta), \tag{88}$$

$$\phi_6(\omega, \zeta) = -\kappa(\lambda_E^2 - \lambda_H^2)\mathcal{F}(\omega + \zeta). \tag{89}$$

λ_E and λ_H are the parameters entered in the normalization conditions

$$\Psi_A(x=0) = \frac{\lambda_E^2}{3}, \quad \Psi_V(x=0) = \frac{\lambda_H^2}{3}. \tag{90}$$

It is known that the EOM, as shown in Eqs. (78–80), imply the connections between the two-particle and three-particle LCDAs,

$$\omega_0 = \lambda_B = \frac{2}{3}\bar{\Lambda}, \quad 2\bar{\Lambda}^2 = 2\lambda_E^2 + \lambda_H^2, \quad \text{Exp - Model}, \tag{91}$$

$$\omega_0 = \frac{5}{2}\lambda_B = 2\bar{\Lambda}, \quad \bar{\Lambda}^2 = 2\lambda_E^2 + \lambda_H^2, \quad \text{LD - model}, \tag{92}$$

with taking the general functions

$$f(\omega) = \frac{1}{\omega_0^2}e^{-\omega/\omega_0}, \quad \text{Exp - Model}, \tag{93}$$

$$f(\omega) = \frac{5}{8\omega_0^5}(2\omega_0 - \omega)^3\Theta[2\omega_0 - \omega], \quad \text{LD - Model}. \tag{94}$$

The normalization constants in these two particular models are

$$\kappa = \frac{1}{3\omega_0^2}, \quad \text{Exp - Model}, \tag{95}$$

$$\kappa = \frac{7}{2\omega_0^2}, \quad \text{LD - Model}. \tag{96}$$

We use the exponential models in our numerical evaluation.

B Coefficients in the three-particle correction

B.1 Correction coefficients to $\mathcal{F}_+(q^2)$

$$\begin{aligned} C_{1,\mathcal{F}_+}^{\Phi_A-\Phi_V} &= -\frac{2u-2}{\bar{\sigma}m_B^2}, \\ C_{2,\mathcal{F}_+}^{\Phi_A-\Phi_V} &= -\frac{(2u-2)(m_B^2 - q^2) + (2u+1)\bar{\sigma}^2m_B^2}{\bar{\sigma}m_B^2}, \\ C_{2,\mathcal{F}_+}^{\Phi_V} &= -6u\bar{\sigma}, \\ C_{2,\mathcal{F}_+}^{\bar{X}_A} &= \frac{(2u-1)}{m_B}, \quad C_{3,\mathcal{F}_+}^{\bar{X}_A} = \frac{2(2u-1)(\bar{\sigma}^2m_B^2 - q^2)}{m_B}, \\ C_{2,\mathcal{F}_+}^{\bar{Y}_A+\bar{W}} &= \frac{18}{m_B}, \quad C_{2,\mathcal{F}_+}^{\bar{X}_A} = \frac{1}{m_B}, \quad C_{2,\mathcal{F}_+}^{\bar{Y}_A} = -\frac{2}{m_B}, \\ C_{3,\mathcal{F}_+}^{\bar{X}_A} &= -8\bar{\sigma} \frac{[2m_S^2\bar{\sigma} + (1-2\sigma)(m_B^2 - m_S^2 - q^2) - 2\sigma q^2]}{m_B}, \end{aligned}$$

$$\begin{aligned}
C_{3,\mathcal{F}_+}^{\bar{Y}_A} &= -C_{3,\mathcal{F}_+}^{\bar{X}_A}, \\
C_{3,\mathcal{F}_+}^{\bar{W}} &= -16\bar{\sigma}(u+u^2) - 4(4u^2+u) \\
&\quad \cdot \frac{[2m_S^2\bar{\sigma} + (1-2\sigma)(m_B^2 - m_S^2 - q^2) - 2\sigma q^2]}{m_B^2}, \quad (97)
\end{aligned}$$

B.2 Correction coefficients to $\mathcal{F}_-(q^2)$

$$\begin{aligned}
C_{1,\mathcal{F}_-}^{\Phi_{A-\Phi_V}} &= -\frac{2u-2}{\bar{\sigma}m_B^2}, \\
C_{2,\mathcal{F}_-}^{\Phi_{A-\Phi_V}} &= -\frac{(2u-2)(m_B^2 - q^2) - (2u+1)\sigma\bar{\sigma}m_B^2}{\bar{\sigma}m_B^2}, \\
C_{2,\mathcal{F}_-}^{\Phi_V} &= 6u\sigma, \\
C_{2,\mathcal{F}_-}^{\bar{X}_A} &= -\frac{3(2u-1)}{m_B}, \\
C_{3,\mathcal{F}_-}^{\bar{X}_A} &= -\frac{2(2u-1)\sigma(\bar{\sigma}^2m_B^2 - q^2)}{\bar{\sigma}m_B}, \\
C_{2,\mathcal{F}_-}^{\bar{Y}_A+\bar{W}} &= \frac{18}{m_B}, \quad C_{2,\mathcal{F}_-}^{\bar{X}_A} = \frac{1}{m_B}, \quad C_{2,\mathcal{F}_-}^{\bar{Y}_A} = -\frac{2}{m_B}, \\
C_{3,\mathcal{F}_-}^{\bar{X}_A} &= 8\sigma \frac{[2m_S^2\bar{\sigma} + (1-2\sigma)(m_B^2 - m_S^2 - q^2) - 2\sigma q^2]}{m_B}, \\
C_{3,\mathcal{F}_-}^{\bar{Y}_A} &= -C_{3,\mathcal{F}_-}^{\bar{X}_A}, \\
C_{3,\mathcal{F}_-}^{\bar{W}} &= 16\sigma(u+u^2) - 4(4u^2+u) \\
&\quad \cdot \frac{[2m_S^2\bar{\sigma} + (1-2\sigma)(m_B^2 - m_S^2 - q^2) - 2\sigma q^2]}{m_B^2}. \quad (98)
\end{aligned}$$

B.3 Correction coefficients to $\mathcal{F}_{T,p}(q^2)$

$$\begin{aligned}
C_{2,\mathcal{F}_{T,p}}^{\Phi_{A-\Phi_V}} &= -\frac{(2u-1)}{m_B}, \quad C_{2,\mathcal{F}_{T,p}}^{\Phi_V} = -\frac{3u}{m_B}, \\
C_{2,\mathcal{F}_{T,p}}^{\bar{X}_A} &= 2\frac{2u-1}{\bar{\sigma}m_B^2}, \\
C_{3,\mathcal{F}_{T,p}}^{\bar{X}_A} &= -2\frac{[(2u-1)(\bar{\sigma}^2m_B^2 - q^2)]}{\bar{\sigma}m_B^2}, \\
C_{2,\mathcal{F}_{T,p}}^{\bar{X}_A} &= -\frac{8}{m_B\sqrt{q^2}}, \\
C_{3,\mathcal{F}_{T,p}}^{\bar{X}_A} &= 4\bar{\sigma} \frac{[\bar{\sigma}(m_B^2 - m_S^2 - q^2) - 2\sigma q^2]}{q^2}, \\
C_{3,\mathcal{F}_{T,p}}^{\bar{W}} &= 3u \left[\frac{\bar{\sigma}}{\sqrt{q^2}} - \frac{(m_B - \sqrt{q^2})}{m_B\sqrt{q^2}} \right], \\
C_{3,\mathcal{F}_{T,p}}^{\bar{Z}} &= (24u^2 + u - 47)
\end{aligned}$$

B.4 Correction coefficients to $\mathcal{F}_{T,q}(q^2)$

$$\begin{aligned}
C_{1,\mathcal{F}_{T,q}}^{\Phi_{A-\Phi_V}} &= \frac{2u-1}{\bar{\sigma}m_B}, \\
C_{2,\mathcal{F}_{T,q}}^{\Phi_{A-\Phi_V}} &= -\frac{(2u-1)[\bar{\sigma}^2m_B^2 - q^2(1-2\sigma)]}{\bar{\sigma}m_B}, \\
C_{1,\mathcal{F}_{T,q}}^{\Phi_V} &= \frac{3u}{\bar{\sigma}m_B}, \quad C_{2,\mathcal{F}_{T,q}}^{\Phi_V} = -\frac{3u[\bar{\sigma}^2m_B^2 - q^2(1-2\sigma)]}{\bar{\sigma}m_B}, \\
C_{1,\mathcal{F}_{T,q}}^{\bar{X}_A} &= -\frac{2(2u-1)}{\bar{\sigma}^2m_B^2}, \quad C_{2,\mathcal{F}_{T,q}}^{\bar{X}_A} = \frac{4\sigma(2u-1)q^2}{\bar{\sigma}^2m_B^2}, \\
C_{3,\mathcal{F}_{T,q}}^{\bar{X}_A} &= 2\frac{[(2u-1)(\bar{\sigma}^2m_B^2 - q^2)][\bar{\sigma}^2m_B^2 - q^2(1-2\sigma)]}{\bar{\sigma}^2m_B^2}, \\
C_{2,\mathcal{F}_{T,q}}^{\bar{X}_A} &= 4 - \frac{16\sqrt{q^2}}{m_B}, \\
C_{3,\mathcal{F}_{T,q}}^{\bar{X}_A} &= 8\sigma[\bar{\sigma}(m_B^2 - m_S^2 - q^2) - 2\sigma q^2], \\
C_{2,\mathcal{F}_{T,q}}^{\bar{Y}_A} &= 120, \\
C_{3,\mathcal{F}_{T,p}}^{\bar{W}} &= 6u \left[\sigma\sqrt{q^2} + \frac{(m_B - \sqrt{q^2})\sqrt{q^2}}{m_B} \right], \\
C_{3,\mathcal{F}_{T,p}}^{\bar{Z}} &= (24u^2 + u - 47) \\
&\quad \cdot \frac{[\bar{\sigma}(m_B^2 - m_S^2 + q^2) - 2(m_B - \sqrt{q^2})\sqrt{q^2}]}{m_B}. \quad (100)
\end{aligned}$$

B.5 Correction coefficients to $\mathcal{F}_0(q^2)$

$$\begin{aligned}
C_{1,\mathcal{F}_0}^{\Phi_{A-\Phi_V}} &= \frac{3(1-2u)}{2\bar{\sigma}m_B}, \\
C_{2,\mathcal{F}_0}^{\Phi_{A-\Phi_V}} &= \frac{3(1-2u)}{2\bar{\sigma}m_B}(\bar{\sigma}^2m_B^2 - q^2), \\
C_{1,\mathcal{F}_0}^{\Phi_V} &= -\frac{3u}{\bar{\sigma}m_B}, \quad C_{2,\mathcal{F}_0}^{\Phi_V} = -\frac{3u}{\bar{\sigma}m_B}(\bar{\sigma}^2m_B^2 - q^2), \\
C_{1,\mathcal{F}_0}^{\bar{X}_A} &= \frac{2u+1}{\bar{\sigma}^2m_B^2}, \\
C_{2,\mathcal{F}_0}^{\bar{X}_A} &= (2u+7) - \frac{2(2u+1)(\bar{\sigma}^2m_B^2 - q^2)}{\bar{\sigma}^2m_B^2}, \\
C_{3,\mathcal{F}_0}^{\bar{X}_A} &= \frac{2u+1}{\bar{\sigma}^2m_B^2}(\bar{\sigma}^2m_B^2 - q^2)^2, \\
C_{2,\mathcal{F}_0}^{\bar{X}_A} &= \frac{3}{2}, \quad C_{3,\mathcal{F}_0}^{\bar{W}} = 9u \left[\bar{\sigma}(m_B - \sqrt{q^2}) - \sigma\sqrt{q^2} \right],
\end{aligned}$$

$$C_{3,\mathcal{F}_0}^{\bar{Z}} = -24u^2 \left[\bar{\sigma}(m_B - \sqrt{q^2}) - \sigma\sqrt{q^2} \right]. \quad (101)$$

References

1. R.R. Horgan, Z. Liu, S. Meinel, M. Wingate, Phys. Rev. Lett. **112**, 212003 (2014). [arXiv:1310.3887](#) [hep-ph]
2. J. A. Bailey et al. [Fermilab Lattice and MILC Collaborations], Phys. Rev. D **92**, no. 1, 014024 (2015). [arXiv:1503.07839](#) [hep-lat]
3. V.M. Braun, I.E. Halperin, Phys. Lett. B **328**, 457 (1994). [arXiv:hep-ph/9402270](#)
4. V. M. Braun, [arXiv:hep-ph/9801222](#)
5. P. Colangelo, A. Khodjamirian, In *Shifman, M. (ed.): At the frontier of particle physics, vol. 3* 1495-1576. [arXiv:hep-ph/0010175](#)
6. P. Ball, R. Zwicky, Phys. Rev. D **71**, 014015 (2005). [arXiv:hep-ph/0406232](#)
7. P. Ball, R. Zwicky, Phys. Rev. D **71**, 014029 (2005). [arXiv:hep-ph/0412079](#)
8. A. Bharucha, D.M. Straub, R. Zwicky, JHEP **1608**, 098 (2016). [arXiv:1503.05534](#) [hep-ph]
9. A. Khodjamirian, T. Mannel, N. Offen, Phys. Rev. D **75**, 054013 (2007). [arXiv:hep-ph/0611193](#)
10. G. Duplancic, A. Khodjamirian, T. Mannel, B. Melic, N. Offen, JHEP **0804**, 014 (2008). [arXiv:0801.1796](#) [hep-ph]
11. Y.M. Wang, Y.L. Shen, Nucl. Phys. B **898**, 563 (2015). [arXiv:1506.00667](#) [hep-ph]
12. S. Cheng, A. Khodjamirian, J. Virto, JHEP **1705**, 157 (2017). [arXiv:1701.01633](#) [hep-ph]
13. S. Descotes-Genon, A. Khodjamirian, J. Virto, JHEP **1912**, 083 (2019). [arXiv:1908.02267](#) [hep-ph]
14. A.V. Rusov, Eur. Phys. J. C **77**(7), 442 (2017). [arXiv:1705.01929](#) [hep-ph]
15. Hn Li, G.F. Sterman, Nucl. Phys. B **381**, 129 (1992)
16. Hn Li, H.L. Yu, Phys. Rev. D **53**, 2480 (1996). [arXiv:hep-ph/9411308](#)
17. T. Kurimoto, H.N.Li, A.I. Sanda, Phys. Rev. D **65**, 014007 (2002). [arXiv:hep-ph/0105003](#)
18. C.D. Lu, M.Z. Yang, Eur. Phys. J. C **28**, 515 (2003). [arXiv:hep-ph/0212373](#)
19. Y.C. Chen, H.N. Li, Phys. Lett. B **712**, 63 (2012). [arXiv:1112.5059](#) [hep-ph]
20. Hn Li, Y.L. Shen, Y.M. Wang, Phys. Rev. D **85**, 074004 (2012). [arXiv:1201.5066](#) [hep-ph]
21. S. Cheng, Y.Y. Fan, X. Yu, C.D. Lü, Z.J. Xiao, Phys. Rev. D **89**(9), 094004 (2014). [arXiv:1402.5501](#) [hep-ph]
22. R.L. Jaffe, Phys. Rev. D **15**, 267 (1977)
23. R.L. Jaffe, Phys. Rev. D **15**, 281 (1977)
24. H.Y. Cheng, C.K. Chua, K.C. Yang, Phys. Rev. D **73**, 014017 (2006). [arXiv:hep-ph/0508104](#)
25. F.E. Close, N.A. Tornqvist, J. Phys. G **28**, R249 (2002). [arXiv:hep-ph/0204205](#)
26. N. N. Achasov, A. V. Kiselev, Phys. Rev. D **73**, 054029 (2006), Erratum: [Phys. Rev. D **74**, 059902 (2006)]. [arXiv:hep-ph/0512047](#)
27. N.N. Achasov, A.V. Kiselev, Phys. Rev. D **83**, 054008 (2011). [arXiv:1011.4446](#) [hep-ph]
28. S. Agaev, K. Azizi, H. Sundu, Phys. Lett. B **781**, 279–282 (2018). [arXiv:1711.11553](#) [hep-ph]
29. S. Agaev, K. Azizi, H. Sundu, Phys. Lett. B **784**, 266–270 (2018). [arXiv:1804.01726](#) [hep-ph]
30. J.D. Weinstein, N. Isgur, Phys. Rev. Lett. **48**, 659 (1982)
31. J.D. Weinstein, N. Isgur, Phys. Rev. D **27**, 588 (1983)
32. J.D. Weinstein, N. Isgur, Phys. Rev. D **41**, 2236 (1990)
33. N. Ghahramany, R. Khosravi, Phys. Rev. D **80**, 016009 (2009)
34. P. Colangelo, F. De Fazio, W. Wang, Phys. Rev. D **81**, 074001 (2010). [arXiv:1002.2880](#) [hep-ph]
35. Y.J. Sun, Z.H. Li, T. Huang, Phys. Rev. D **83**, 025024 (2011). [arXiv:1011.3901](#) [hep-ph]
36. Z.G. Wang, Eur. Phys. J. C **75**(2), 50 (2015). [arXiv:1409.6449](#) [hep-ph]
37. B.H. Behrens et al. [CLEO Collaboration], Phys. Rev. D **61**, 052001 (2000). [arXiv:hep-ex/9905056](#)
38. N. E. Adam et al. [CLEO Collaboration], Phys. Rev. Lett. **99**, 041802 (2007). [arXiv:hep-ex/0703041](#) [HEP-EX]
39. M.A. Shifman, A.I. Vainshtein, V.I. Zakharov, Nucl. Phys. B **147**, 385 (1979)
40. A. Gokalp, Y. Sarac, O. Yilmaz, Phys. Lett. B **609**, 291 (2005). [arXiv:hep-ph/0410380](#)
41. A.V. Anisovich, V.V. Anisovich, V.A. Nikonov, Eur. Phys. J. A **12**, 103 (2001). [arXiv:hep-ph/0108186](#)
42. H.Y. Cheng, Phys. Rev. D **67**, 034024 (2003). [arXiv:hep-ph/0212117](#)
43. R. Kaminski, G. Mennessier, S. Narison, Phys. Lett. B **680**, 148 (2009). [arXiv:0904.2555](#) [hep-ph]
44. G. Mennessier, S. Narison, X.G. Wang, Phys. Lett. B **688**, 59 (2010). [arXiv:1002.1402](#) [hep-ph]
45. Z.Q. Zhang, J.D. Zhang, Eur. Phys. J. C **67**, 163 (2010). [arXiv:1004.4426](#) [hep-ph]
46. J.W. Li, D.S. Du, C.D. Lu, Eur. Phys. J. C **72**, 2229 (2012). [arXiv:1212.5987](#) [hep-ph]
47. Z. Q. Zhang, S. Y. Wang, X. K. Ma, Phys. Rev. D **93**, no. 5, 054034 (2016). [arXiv:1601.04137](#) [hep-ph]
48. X. Liu, Z. T. Zou, Y. Li, Z. J. Xiao, Phys. Rev. D **100**(1), 013006 (2019). [arXiv:1906.02489](#) [hep-ph]
49. T. Feldmann, P. Kroll, B. Stech, Phys. Lett. B **449**, 339 (1999). [arXiv:hep-ph/9812269](#)
50. M. Tanabashi et al. [Particle Data Group], Phys. Rev. D **98**(3), 030001 (2018)
51. J. Govaerts, L.J. Reinders, F. de Viron, J. Weyers, Nucl. Phys. B **283**, 706 (1987)
52. C. Becchi, S. Narison, E. de Rafael, F.J. Yndurain, Z. Phys. C **8**, 335 (1981)
53. H. Leutwyler, Phys. Lett. B **378**, 313 (1996). [arXiv:hep-ph/9602366](#)
54. B.L. Ioffe, Phys. Atom. Nucl. **66**, 30 (2003)
55. B.L. Ioffe, Yad. Fiz. **66**, 32 (2003). [arXiv:hep-ph/0207191](#)
56. V.L. Chernyak, A.R. Zhitnitsky, JETP Lett. **25**, 510 (1977)
57. V.L. Chernyak, A.R. Zhitnitsky, Pisma. Zh. Eksp. Teor. Fiz. **25**, 544 (1977)
58. G.P. Lepage, S.J. Brodsky, Phys. Lett. B **87**, 359 (1979)
59. J.A.M. Vermaseren, S.A. Larin, T. van Ritbergen, Phys. Lett. B **05**, 327 (1997). [arXiv:hep-ph/9703284](#)
60. R. Aaij et al. [LHCb Collaboration], Phys. Rev. D **89**(9), 092006 (2014). [arXiv:1402.6248](#) [hep-ex]
61. B. Geyer, O. Witzel, Phys. Rev. D **72**, 034023 (2005). [arXiv:hep-ph/0502239](#)
62. V.M. Braun, Y. Ji, A.N. Manashov, JHEP **1705**, 022 (2017). [arXiv:1703.02446](#) [hep-ph]
63. M. Beneke, V.M. Braun, Y. Ji, Y.B. Wei, JHEP **1807**, 154 (2018). [arXiv:1804.04962](#) [hep-ph]
64. N. Gubernari, A. Koku, D. van Dyk, JHEP **1901**, 150 (2019). [arXiv:1811.00983](#) [hep-ph]
65. C.D. Lü, Y.L. Shen, Y.M. Wang, Y.B. Wei, JHEP **1901**, 024 (2019). [arXiv:1810.00819](#) [hep-ph]
66. Y.L. Shen, Z.T. Zou, Y.B. Wei, Phys. Rev. D **99**(1), 016004 (2019). [arXiv:1811.08250](#) [hep-ph]
67. M. Wirbel, B. Stech, M. Bauer, Z. Phys. C **29**, 637 (1985)
68. M. Bauer, B. Stech, M. Wirbel, Z. Phys. C **34**, 103 (1987)

69. Y.L. Shen, Z.J. Yang, X. Yu, Phys. Rev. D **90**(11), 114015 (2014). [arXiv:1207.5912](#) [hep-ph]
70. A. Bazavov et al. [Fermilab Lattice and MILC Collaborations], Phys. Rev. D **85**, 114506 (2012). [arXiv:1112.3051](#) [hep-lat]
71. P. Gelhausen, A. Khodjamirian, A. A. Pivovarov, D. Rosenthal, Phys. Rev. D **88**, 014015 (2013), Erratum: [Phys. Rev. D **89**, 099901 (2014)], Erratum: [Phys. Rev. D **91**, 099901 (2015)]. [arXiv:1305.5432](#) [hep-ph]
72. J. Gao, C. D. Lü, Y. L. Shen, Y. M. Wang, Y. B. Wei, [arXiv:1907.11092](#) [hep-ph]
73. A. Khodjamirian, T. Mannel, N. Offen, Y.-M. Wang, Phys. Rev. D **83**, 094031 (2011). [arXiv:1103.2655](#) [hep-ph]
74. R.H. Li, C.D. Lu, W. Wang, X.X. Wang, Phys. Rev. D **79**, 014013 (2009). [arXiv:0811.2648](#) [hep-ph]
75. B. El-Bennich, O. Leitner, J.-P. Dedonder, B. Loiseau, Phys. Rev. D **79**, 076004 (2009). [arXiv:0810.5771](#) [hep-ph]
76. A. Issadykov, M.A. Ivanov, S.K. Sakhiyev, Phys. Rev. D **91**(7), 074007 (2015). [arXiv:1502.05280](#) [hep-ph]
77. J.F. Donoghue, J. Gasser, H. Leutwyler, Nucl. Phys. B **343**, 341 (1990)
78. F.J. Yndurain, Phys. Lett. B **612**, 245 (2005). [arXiv:hep-ph/0501104](#)
79. J.R. Pelaez, F.J. Yndurain, Phys. Rev. D **71**, 074016 (2005). [arXiv:hep-ph/0411334](#)
80. R. Kaminski, J.R. Pelaez, F.J. Yndurain, Phys. Rev. D **77**, 054015 (2008). [arXiv:0710.1150](#) [hep-ph]
81. R. Garcia-Martin, R. Kaminski, J.R. Pelaez, J. Ruiz de Elvira, F.J. Yndurain, Phys. Rev. D **83**, 074004 (2011). [arXiv:1102.2183](#) [hep-ph]
82. X.W. Kang, B. Kubis, C. Hanhart, U.G. Meißner, Phys. Rev. D **89**, 053015 (2014). [arXiv:1312.1193](#) [hep-ph]
83. J.M. Yuan, Z.F. Zhang, T.G. Steele, H.Y. Jin, Z.R. Huang, Phys. Rev. D **96**(1), 014034 (2017). [arXiv:1705.00397](#) [hep-ph]
84. U.G. Meißner, J.A. Oller, Nucl. Phys. A **679**, 671 (2001). [arXiv:hep-ph/0005253](#)
85. T.A. Lahde, U.G. Meißner, Phys. Rev. D **74**, 034021 (2006). [arXiv:hep-ph/0606133](#)
86. M. Döring, U. G. Meißner, W. Wang, JHEP **1310**, 011 (2013). [arXiv:1307.0947](#) [hep-ph]
87. U.G. Meißner, W. Wang, Phys. Lett. B **730**, 336 (2014). [arXiv:1312.3087](#) [hep-ph]
88. C. Hanhart, Phys. Lett. B **715**, 170–177 (2012). [arXiv:1203.6839](#) [hep-ph]
89. S. Ropertz, C. Hanhart, B. Kubis, Eur. Phys. J. C **78**(12), 1000 (2018). [arXiv:1809.06867](#) [hep-ph]
90. S. Cheng and Q. Qin, Phys. Rev. D **99**, no. 1, 016019 (2019). [arXiv:1810.10524](#) [hep-ph]
91. L.Y. Dai, M.R. Pennington, Phys. Rev. D **90**(3), 036004 (2014). [arXiv:1404.7524](#) [hep-ph]
92. L.Y. Dai, U.G. Meißner, Phys. Lett. B **783**, 294 (2018). [arXiv:1706.10123](#) [hep-ph]
93. P. Buettiker, S. Descotes-Genon, B. Moussallam, Eur. Phys. J. C **33**, 409 (2004). [arXiv:hep-ph/0310283](#)
94. S. Faller, T. Feldmann, A. Khodjamirian, T. Mannel, D. van Dyk, Phys. Rev. D **89**(1), 014015 (2014). [arXiv:1310.6660](#) [hep-ph]
95. S.M. Flatte, M. Alston-Garnjost, A. Barbaro-Galtieri, J.H. Friedman, G.R. Lynch, S.D. Protopopescu, M.S. Rabin, F.T. Solmitz, Phys. Lett. **38B**, 232 (1972)
96. S.M. Flatte, Phys. Lett. **63B**, 228 (1976)
97. C. Bourrely, I. Caprini, L. Lellouch, Phys. Rev. D **79**, 013008 (2009), Erratum: [Phys. Rev. D **82**, 099902 (2010)]. [arXiv:0807.2722](#) [hep-ph]
98. S. Cheng, Phys. Rev. D **99**(5), 053005 (2019). [arXiv:1901.06071](#) [hep-ph]
99. C. Hambrook, A. Khodjamirian, Nucl. Phys. B **905**, 373 (2016). [arXiv:1511.02509](#) [hep-ph]
100. S. Cheng, A. Khodjamirian, J. Virto, Phys. Rev. D **96**(5), 051901 (2017). [arXiv:1709.00173](#) [hep-ph]
101. A.G. Grozin, M. Neubert, Phys. Rev. D **55**, 272 (1997). [arXiv:hep-ph/9607366](#)